AD-A079 311 NAVAL RESEARCH LAB WASHINGTON DC F/G 18/4
DETECTION AND MONITORING OF AIRBORNE NUCLEAR WASTE MATERIALS. A--ETC(U)
DEC 79 J R MCDONALD , A P BARONAVSKI DE-AI05-7641501
UNCLASSIFIED NRL-MR-4125 SBIE -AD-E000 346. NL

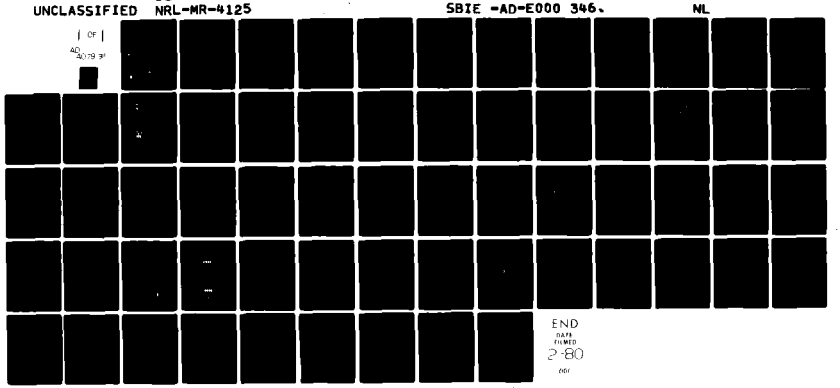

NRL Memorandum Report 4125

Detection and Monitoring of Airborne Nuclear Waste Materials

Annual Report to the Department of Energy

J. R. McDonald, A. P. Baronavski, L. R. Pasternack-Rafferty and V. M. Donnelly

Chemical Diagnostics Branch
Chemistry Division

December 4, 1979

NAVAL RESEARCH LABORATORY
Washington, D.C.

SECURITY CLASSIFICATION OF THIS PAGE (When Data Entered)

(9) **REPORT DOCUMENTATION PAGE**

READ INSTRUCTIONS BEFORE COMPLETING FORM

1. REPORT NUMBER	2. GOVT ACCESSION NO.	3. RECIPIENT'S CATALOG NUMBER
NRL Memorandum Report 4125		

(6) **DETECTION AND MONITORING OF AIRBORNE NUCLEAR WASTE MATERIALS, ANNUAL REPORT TO DEPARTMENT OF ENERGY**

5. TYPE OF REPORT & PERIOD COVERED: Annual report on continuing Department of Energy problem.

6. PERFORMING ORG. REPORT NUMBER

(15) 7. AUTHOR(s): (10) J. R. McDonald, A. P. Baronavski, L. R. Pasternack-Rafferty and V. M. Donnelly

8. CONTRACT OR GRANT NUMBER(s): DE-AI05-76ER01541

9. PERFORMING ORGANIZATION NAME AND ADDRESS: Naval Research Laboratory, Washington, DC 20375

10. PROGRAM ELEMENT, PROJECT, TASK AREA & WORK UNIT NUMBERS: NRL Problem 61-0009-0-0

11. CONTROLLING OFFICE NAME AND ADDRESS: Department of Energy, WPR Branch, Gaithersburg, Maryland (Mr. Jack Dempsey)

(11) 12. REPORT DATE: December 4, 1979

13. NUMBER OF PAGES: 62

14. MONITORING AGENCY NAME & ADDRESS (if different from Controlling Office): Department of Energy, Oak Ridge Operations Office, Oak Ridge, TN 37834 (Mr. Dewey Large)

(12) 63

15. SECURITY CLASS. (of this report): UNCLASSIFIED

15a. DECLASSIFICATION/DOWNGRADING SCHEDULE

16. DISTRIBUTION STATEMENT (of this Report)

Approved for public release; distribution unlimited.

17. DISTRIBUTION STATEMENT (of the abstract entered in Block 20, if different from Report)

(14) NRL-MR-4125

18. SUPPLEMENTARY NOTES

(18) SBIE (19) AD-E000 346

19. KEY WORDS (Continue on reverse side if necessary and identify by block number)

Tritium
Lasers
Carbon-14
Optical diagnostics
Iodine-129
Airborne nuclides

20. ABSTRACT (Continue on reverse side if necessary and identify by block number)

The Chemistry Division of the Naval Research Laboratory in cooperation with the Department of Energy is carrying out research related to detection and monitoring of several airborne species associated with nuclear facilities. Laser fluorescence Iodine-129 measurement techniques have been developed for batch processing as well as continuous monitoring. A commerical prototype has been procured and evaluated. An optical detection scheme for measurement of airborne tritium has been evaluated and further recommendations made. An optical diagnostic for measurement of airborne

(Continues)

DD FORM 1 JAN 73 1473 EDITION OF 1 NOV 65 IS OBSOLETE
S/N 0102-014-6601

SECURITY CLASSIFICATION OF THIS PAGE (When Data Entered)

251950

20. Abstract (Continued)

Carbon-14 has been procured and preliminary testing indicates an ultimate sensitivity of one part per trillion. Extensions of this technique to isotopes other than Carbon-14 are feasible, especially regarding HTO, NO_2^-, and $N_2^{15}O$.

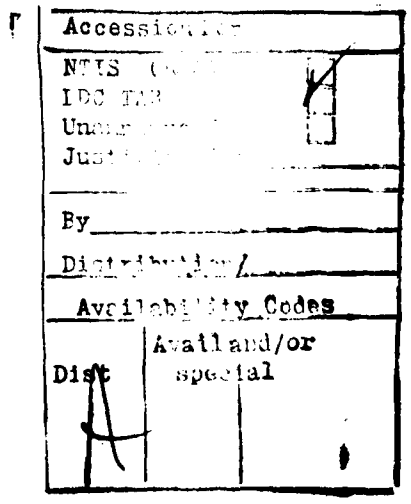

TABLE OF CONTENTS

TABLE OF CONTENTS (CONT'D)

LIST OF ILLUSTRATIONS

LIST OF TABLES

Preface

This annual report is prepared by Code 6110 of the Chemistry Division of the Naval Research Laboratory under contract with the Department of Energy Interagency Agreement No. DE-AI05-7641501 (formerly No. EY-76-C-05-5057). The research reported in this document covers tasks associated with the project "Detection and Monitoring of Airborne Nuclear Waste Materials". The research was conducted by J. R. McDonald, A. P. Baronavski, L. R. Pasternack-Rafferty and V. M. Donnelly. Research involved in the other project included in this Interagency Agreement, "Development of Solid Adsorbants for Control of Nuclear Plant Off-Gas," (KZ-03-04-03) by V. R. Dietz and J. B. Romans is being reported in a separate document.

SECTION I

1.0 INTRODUCTION

The handling, storage, use, and disposal of nuclear materials requires particular attention to the confinement of these species and prevention of their release to the environment within carefully defined limits. Of particular concern are the airborne nuclear materials, since they often occur in a highly diluted form in extremely large volumes of gas which make their monitoring and removal difficult. Under contract with DoE the NRL Chemistry Division has been carrying out research on various aspects of airborne nuclear materials.

Airborne nuclear materials include a wide range of species such as the atomic rare gases and molecular species such as iodine, iodides and tritium and carbon (14) containing molecules. The monitoring and measurement of radio-nuclides has traditionally relied upon radio-counting techniques in which the physical and chemical form of the airborne material during measurement is not particularly important. With the advent of application of optical detection techniques to some of these materials, the molecular form of the species must be given special attention. Three separate projects are covered in this report relating to developmental research for optical detection of carbon (14), iodine (129), and tritium.

It is intended that this report contain all pertinent information relating to each of the subtasks developed during the contract period FY79. It is assumed that the reader has access to NRL Memorandum Report 3895 of December 1978 which is the year end annual report covering FY78 progress in these task areas.

Note: Manuscript submitted October 16, 1979.

This report is organized into stand-alone sections relating to each of the specie detection subtasks. Portions of the information contained herein have been included in periodic interim reports of progress (mainly as NRL letter reports) during FY79.

SECTION II

A RADIOIODINE DETECTOR BASED ON LASER INDUCED FLUORESCENCE

2.1 INTRODUCTION

Of the six major iodine isotopes produced in nuclear reactors, ^{129}I represents only about 1% of the main fission product iodine isotope yield.[1] Although this isotope has the lowest specific activity and the lowest energy decay products, after a short period of cooling outside the reactor, the major iodine isotope present is ^{129}I. Because ^{129}I has a decay half-life of about 17 million years, new attention has been directed to its cumulative effects.[2,3] In spent fuel processing ^{129}I will have to be recovered and stored indefinitely because of its longevity. Because of the low specific activity, low energy decay products, and because ^{129}I is a minor iodine isotopic constituent in an active core, its detection by counting techniques is often slow and impractical.

For these reasons NRL under contract with DoE undertook developmental research to design an optical detector for I (129). During FY77 a laboratory breadboard detector was fabricated and tested. This system employed laser induced fluorescence using a ^{3}He-^{22}Ne laser source for excitation. The technique was specific for the I (129) isotope and showed a sensitivity in the range of 10^{-10} g/cm^3 of I_2.

During FY78 further developmental work was carried out and specifications were drawn up and a contract let for the fabrication of a commercial prototype detector. The laboratory development and subsequent prototype design and specification are described in earlier reports.[4,5,6]

2.2 EVALUATION OF PROTOTYPE DETECTOR

The $^{129}I_2$ prototype detector from Bendix Corporation was received at NRL in January 1979 after having been returned to the factory for design modifications because the signal processing capability failed to meet specifications. As accepted, the detector uses a Bulova tuning fork light chopper for laser modulation, a PAR Model 124A lock-in amplifier for signal measurement and a PAR Model 123 A.C. offset nulling device to zero scattered light and cell fluorescence. With these signal processing modifications, NRL accepted the instrument after routine quality control and sensitivity evaluations.

2.2.1 Acceptance Testing

Tests were made with both static cells containing $^{129}I_2$ and with flowing tests using $^{127}I_2$ to determine the operating capabilities and effective limits of sensitivity of the equipment.

2.2.2 Static Cell Tests Using $^{129}I_2$

Most of the $^{129}I_2$ cells prepared at NRL and shipped to Bendix for use by Bendix in testing the instrument during design and construction, were broken during operation and shipping prior to arrival at NRL in January 1979. Because $^{129}I_2$ was not available at NRL to construct further cells immediately after receipt of equipment, we have relied on tests made by J. R. McDonald at Bendix in Baltimore prior to shipping of the equipment to NRL. Figure 1 shows the instrument responses for $^{129}I_2$ in evacuated cells in concentrations ranging between 2×10^{-9} and 6×10^{-7} g/cm^3. The instrument response is linear over this concentration range, and signals can be easily measured with the cell of lowest concentration.

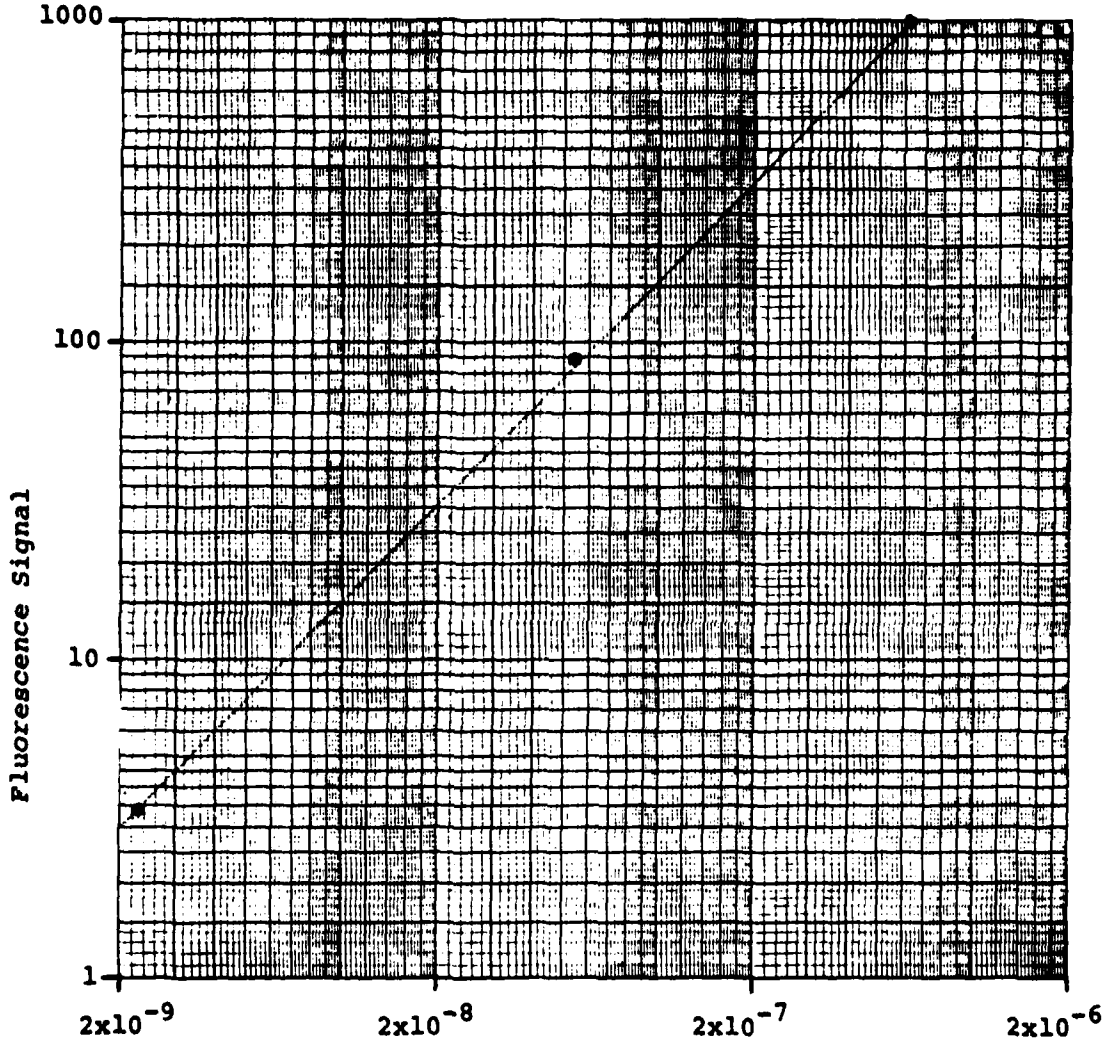

Fig. 1 - Radioiodine prototype detector response for Iodine (129) in static evacuated cells.

2.2.3 Flowing Tests

The flowing tests can much more easily be made using $^{127}I_2$ because there are no radiation problems associated with its handling and because it is relatively easy to control airborne concentrations by use of a permeation tube source. For flowing tests we use a $CH_3{}^{127}I$ permeation tube which is thermostated in a controlled flow oven. The permeation tube produces 1.44 μg/min CH_3I at 35°C. This CH_3I is converted to molecular iodine quantitatively in a quartz tube pyrolysis oven at ∿700°C in flowing streams of air or of He. The $^{127}I_2$ concentrations can be varied by diluting the carrier stream containing the $^{127}I_2$ using calibrated flow meters. Figure 2 shows a plot of measured $^{127}I_2$ signal vs. iodine concentration between 2 and 100 ng iodine/cm^3 in flowing He. The lowest concentrations measured are limited by the ability to make accurate dilutions with the calibrated flow meters. It should be noted that these signals are for $^{127}I_2$ (not $^{129}I_2$) and are in helium (not air) gas. The instrument sensitivity is much greater for $^{129}I_2$ than for $^{127}I_2$. This is partially offset by the increased sensitivity for iodine detection in helium rather than air. When making flowing measurements using $^{127}I_2$, it is necessary to use He rather than air for a carrier gas because of the decreased instrument sensitivity for the stable $^{127}I_2$ isotope.

After these tests, the instrument was deemed as acceptable under the specifications of the NRL contract with Bendix. It was clear that the sensitivity met 10^{-10} g/cm^3 $^{129}I_2$ which was the design specification under which the instrument was purchased.

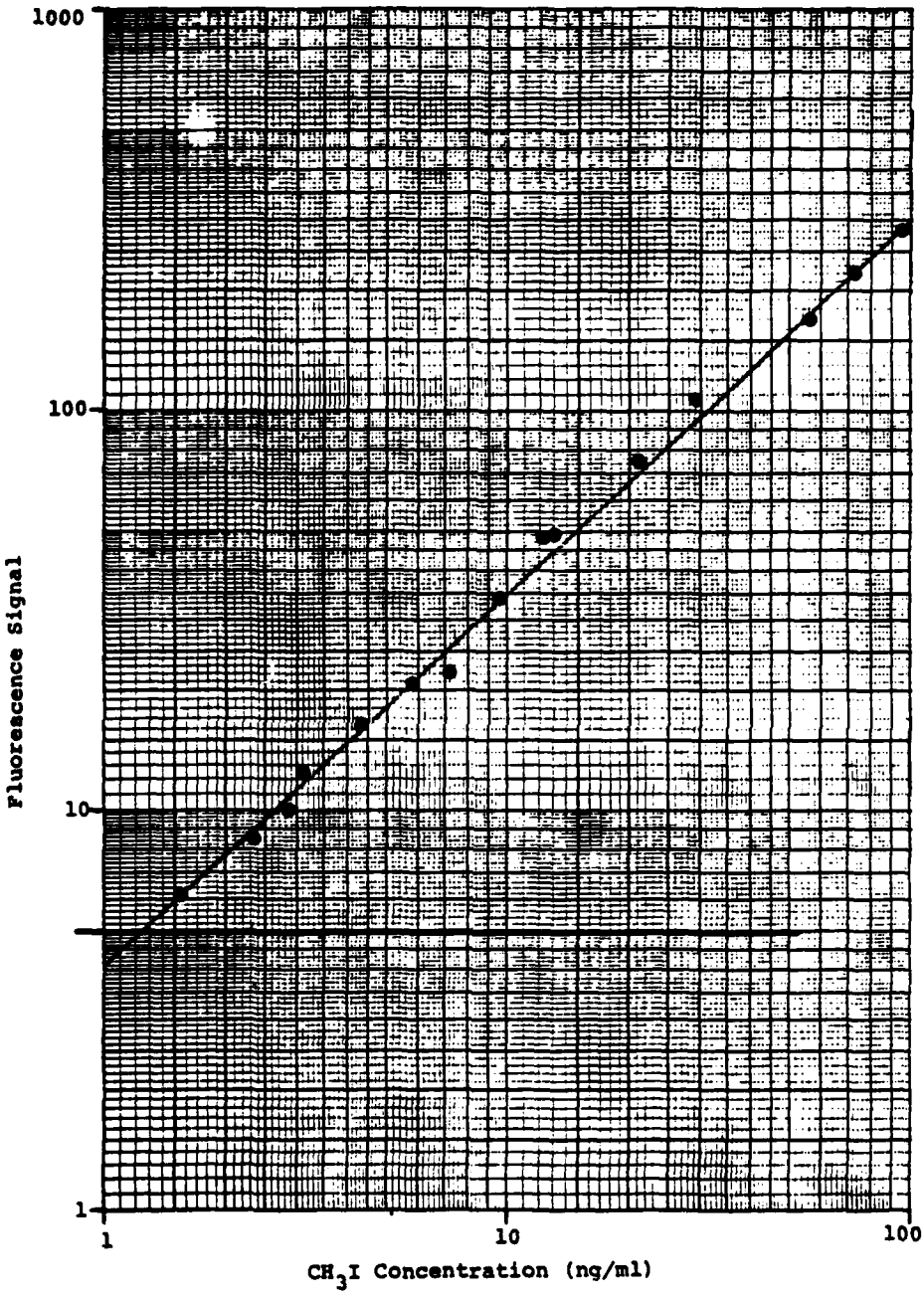

Fig. 2 - Radioiodine prototype detector response for I (127) from pyrolysis of methyliodide in flowing gas cell measurements.

2.3 FIELD TESTING CONSIDERATIONS

Correspondence with Dr. David C. Hetzer of Allied Chemical at the INEL Idaho Falls facility specified for field testing of the detector have clarified current operating parameters at the test stations available for use. The maximum probable ^{129}I concentrations at the APS Sampling Station of $\lesssim 10^{-8}$ $\mu Ci/m^3$ correspond to $\sim 1.3 \times 10^{-14}$ g/cm^3 of $I_2(129)$. At this sampling point, the NO_2 concentration is on the order of a few tenths of a percent. Because each of these levels are well outside the guidelines expected when the instrument specifications were set for construction of the prototype, we have reevaluated the suitability of the prototype for field testing at Idaho Falls.

2.3.1 Extension of Sensitivity for Flowing Operation

The prototype instrument was designed such that it should be possible to considerably extend its sensitivity. The driving potential on the photomultipliers was increased to 1600v which increased the measured signals by approximately a factor of three. The increase results in a dark current and scattered light signal current of $\sim$20 n amp. This is well within the operating capability of the detectors. The A.C. offset modules in the lock-in detectors were included in the design stage to enable the user to null this signal and to continue to operate at lower signal levels with the lock-in detectors. Nearly three orders of magnitude in additional sensitivity are available in this mode over the signals which are measured at concentrations of 10^{-10} g/cm^3. It is not possible to realize all of this potential sensitivity enhancement because of instabilities in the Bulova chopper and because of short-term jitter in the He-Ne laser intensity. Currently,

enhanced sensitivity in this mode at higher P.M. biasing yields about a factor of fifty improvement over the 10^{-10} g/cm^3 design specification for the prototype. Further enhancement could likely be realized by modification of some of the instrument components. This has not been pursued because:

a. This would give a sensitivity limit in excess of 10^{-13} g/cm^3 which falls short of the maximum probable concentration at the APS test station; and

b. Interference problems from the ∿5000 ppm NO_2 present in the gas sample represent a more serious measurement constraint.

2.4 NO_2 INTERFERENCE EVALUATION

Measurements have been made using the Bendix prototype to determine instrument response to flowing gas samples containing NO_2. In Figure 2 the solid horizontal line represents the instrument response to NO_2 present at a concentration of 0.3% (3000 ppm) in the flowing mode. This indicates that 0.3% NO_2 will represent a serious interference with $^{129}I_2$ measurements at $^{129}I_2$ concentrations less than ∿3 ng/cm^3.

Experiments were carried out to determine if the interference of NO_2 could be reduced by use of the in-place quartz pyrolysis oven immediately proceeding the fluorescence sample cell. The quartz pyrolysis oven at 700°C would be expected to completely destroy the NO_2 to form $NO + \frac{1}{2}O_2$. The reverse reaction to reform NO_2 must be either three body or wall catalyzed and, therefore, might be expected to be slow at the lower temperatures outside the oven. Under normal operating conditions of temperature and flow, the NO_2 fluorescence signal is reduced by 20% in flowing airstreams and by a factor of ten in flowing

helium. This level of catalytic destruction of NO_2 is not adequate for use of the prototype detector for field testing at Idaho Falls.

2.5 MIDYEAR OBSERVATIONS AND RECOMMENDATIONS

The Bendix prototype detector after testing and modification operates routinely at the design specification limits. If test sites can be identified which have:

a. I (129) levels $\gtrsim 10^{-10}$ g/cm^3; and

b. NO_2 levels <100 ppm,

the prototype detector is capable of operating on site as a real time detector for flowing gas sampling.

Alternatively, the monitor should be capable of operating as a sensitive test instrument for determining I (129) loadings on filter scrubbing materials in use at nuclear facilities. The iodine can be stripped from the filter materials, either charcoals or zeolites, and total loadings measured with the use of the prototype detector.

Because the ambient concentrations of $^{129}I_2$ at the APS test station fall 10^2-10^5 below the operating limits of the Bendix prototype detector and because of the serious NO_2 interference complications at mid year, we recommended that the prototype detector not be transferred to Idaho Falls for field operations. We proposed that the prototype detector remain at NRL and modifications be undertaken to extend the instrument sensitivity and that techniques be developed to separate the NO_2 and I_2 components in the sampled airstream prior to the optical detection of the iodine.

2.6 BATCH PROCESSING WITH THE PROTOTYPE DETECTOR

At mid year we undertook developmental work to defeat the NO_2

interference and extend the sensitivity to the detection required for use of the iodine detector at INEL. The most promising techniques to accomplish both these objectives involve batch processing of the sample airstream. In this mode relatively large gas samples can be scrubbed to concentrate the iodine in the effluent and discriminate against NO_2 either in the scrubbing or stripping steps. By stripping the concentrated I_2 from the adsorbent phase in helium carrier gas approximately a factor of forty in sensitivity can be realized over measurements in air. This enhancement is in addition to the increased sensitivity to be realized from concentrating the iodine on the scrubber material. Figure 3 shows a block diagram of the experimental setup used for batch processing studies.

The test gas to be scrubbed is introduced at the sample gas inlet. Typically methyl iodide, diluted in air or helium, is used to introduce iodine into the system. Methyl iodide is taken from a permeation tube in a thermostated oven which delivers 1.44 μg of CH_3I/minute. The methyl iodide is quantitatively converted to I_2 in the quartz tube catalytic oven, and is removed from the gas stream in the adsorbent bed contained in the stripping oven. The scrubbed sample gas exits the system via the discharge port. To remove the iodine from the adsorbent bed Stopcocks I and II are rotated to introduce the stripping gas at the stripping gas inlet port. The stripping gas flows counter current to the sample gas flow through the adsorbent bed and quartz catalytic oven to the sample flow cell in the iodine detector. The methyliodide used in the experiments is $CH_3{}^{127}I$. The detector has reduced sensitivity for this isotope, because experiments are easier to carry out with the stable isotope.

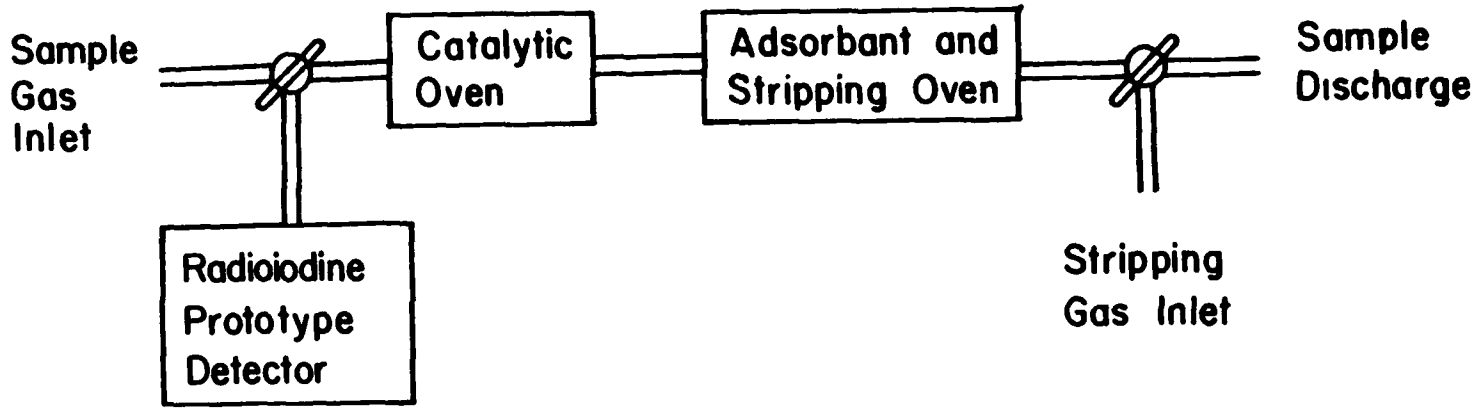

Fig. 3 - Block diagram of apparatus used for batch processing of radioiodine. The sample is flowed through the catalytic oven and is then adsorbed in the second oven. The sample is then removed by back flowing with a stripping gas (He) at an elevated temperature in the stripping oven and sent to the detector.

The two most likely candidates for scrubbing materials are charcoal and various forms of zeolites. Both are known to be efficient filter materials for iodine scrubbing. Two objectives must be realized for their use in this application:

a. A suitable technique must be found for quantitative removal of molecular iodine from the filter substrate; and

b. The filter material chosen must be capable of demonstrating discrimination against NO_2 in either the scrubbing or stripping steps.

2.6.1 Experiments With Charcoal Filters

2.6.1.1 Iodine on Charcoal

A commercial cocoanut charcoal, 40/50 mesh, is loaded into the tube used as the adsorbent bed. The iodine is loaded onto the bed from either flowing air or flowing helium streams. Results are identical in either case. To remove the iodine from the adsorbent a helium counter current flow (30 ml/minute) is used. The oven surrounding the stripper bed is programmed to rapidly rise to 400°C. The quartz pyrolysis oven is maintained at 700-800°C to convert organic iodides which may be stripped from the iodine loaded charcoal. Figure 4 shows a typical run of three repetitions of deposit and removal of iodine. Results are highly repeatable. In these experiments 7 µgrams of CH_3I are used for loading on the charcoal. During the stripping step the iodine begins to strongly desorb at ∿200°C and is entirely removed by ∿380°C. Further cycling of the charcoal does not desorb any additional detectible iodine. Individual adsorbent beds have been cycled through more than fifty repetitions with no noticeable change in efficiency.

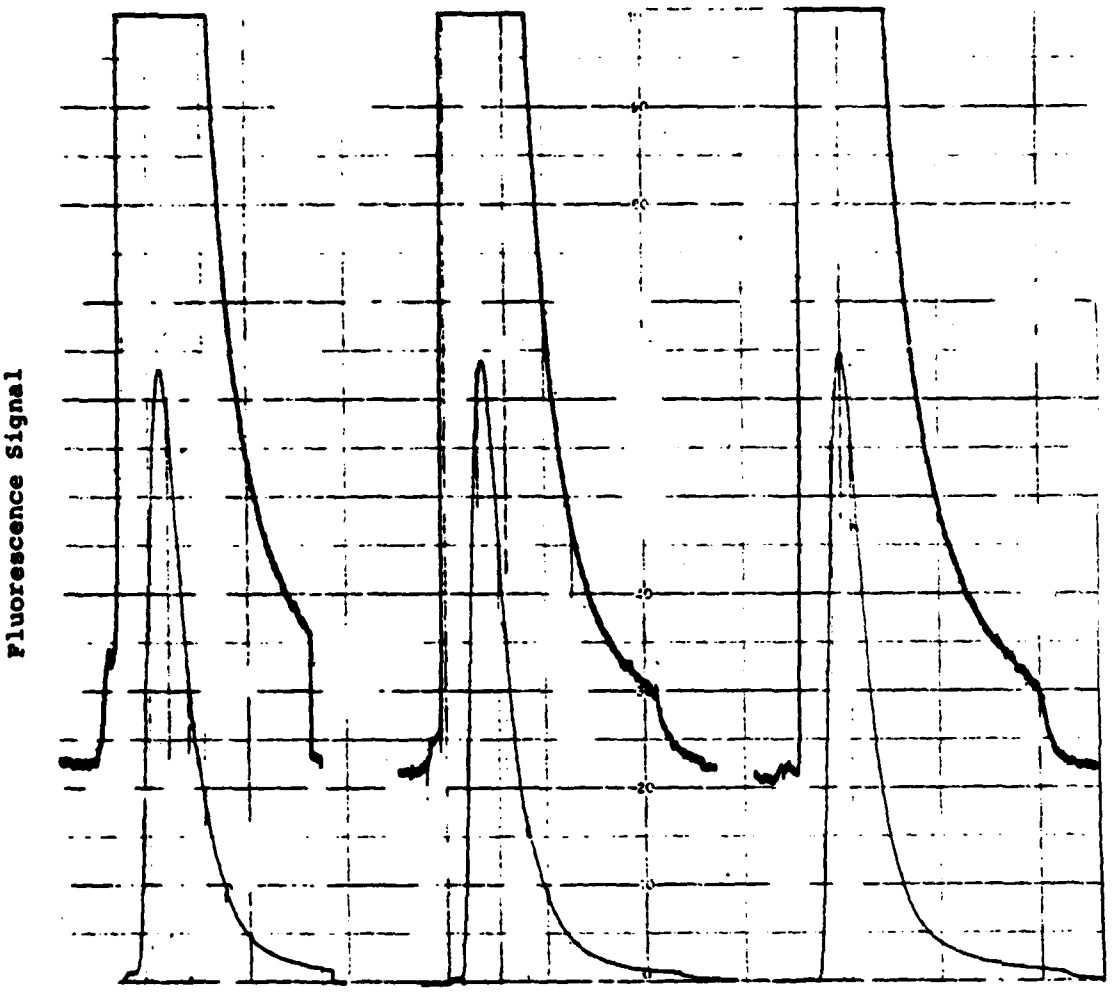

Fig. 4 - Temperature-time histogram for desorption of iodine from charcoal adsorber beds. Three repetitions are shown. In each case seven micrograms of CH_3I is pyrolized to I_2 and deposited in the adsorber bed. Iodine begins to desorb at 200°C and is completely desorbed by 380°C. The upper curve in each plot is at ten times increased sensitivity over the lower curve. See the text for details.

Cocoanut charcoal works efficiently as an adsorbent material for concentrating iodine and with the pyrolyzer organic iodides, are also converted. In addition iodine can be quantitatively recovered from the adsorbent in a counter current flow of helium for optical detection.

2.6.1.2 NO_2 on Charcoal

Experiments were carried out to determine the behavior of the charcoal scrubber in NO_2 containing airstreams. Figure 5 shows the results of a typical experiment. A sample of 0.1% NO_2 in air was deposited at 30 ml/min for ten minutes on the charcoal adsorbent. Figure 5 shows the response of the detector to the eluted NO_2 as a function of oven temperature using helium as a scrubber gas. NO_2 also binds well to charcoal. There are apparently two types of binding sites; one desorbs with a temperature maximum of $\sim 170^{\circ}C$ and the second desorbs with a maximum at $\sim 230^{\circ}C$.

Both iodine and NO_2 show a similar affinity for charcoal in the scrubber. In addition, the NO_2 shows desorption isotherms which are similar to I_2. It appears unlikely that charcoal can be developed for use in this application because of the similar affinity of I_2 and NO_2 for the substrate.

2.6.2 Zeolite Thermal Desorption Experiments

2.6.2.1 Silver Mordenite

Several samples of silver form zeolites have been investigated for suitability as adsorbents to be used with the radioiodine detector. All of these materials are known to be very efficient iodine adsorbers. Gas samples were treated in a similar manner to that described in the previous section using charcoal. Figure 6 shows a thermal desorption curve for

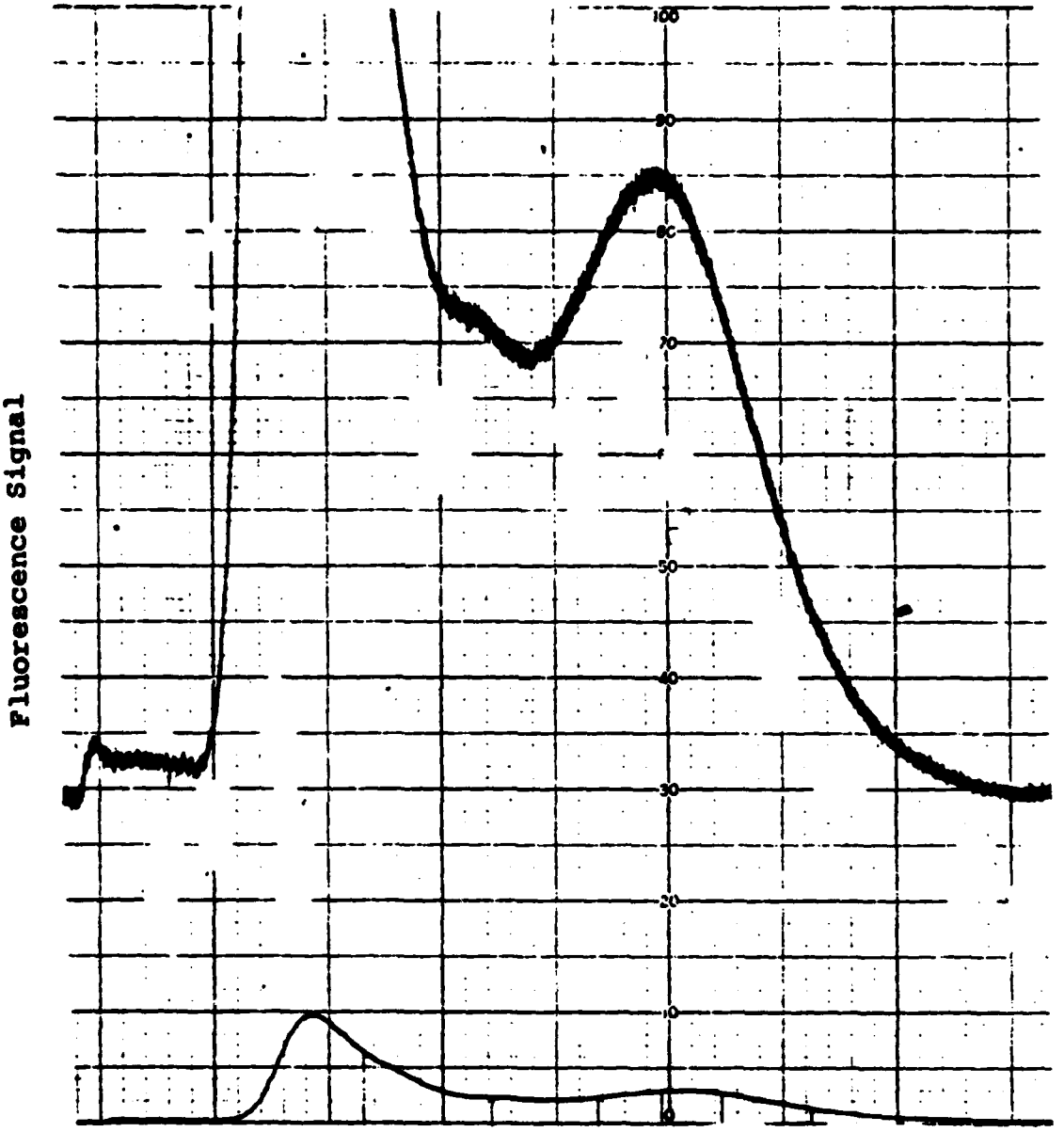

Fig. 5 - Temperature-time histogram for the desorption of NO_2 from the charcoal adsorber bed. 300 ml of 0.1% NO_2 in air was deposited on the bed. Desorbed NO_2 is detected with the radioiodine detector under the same operating conditions as shown in Fig. 2. NO_2 begins to strongly desorb at 150°C and is completely desorbed by 350°C. The upper curve in the figure is at 25 times the sensitivity of the lower curve. See the text for details.

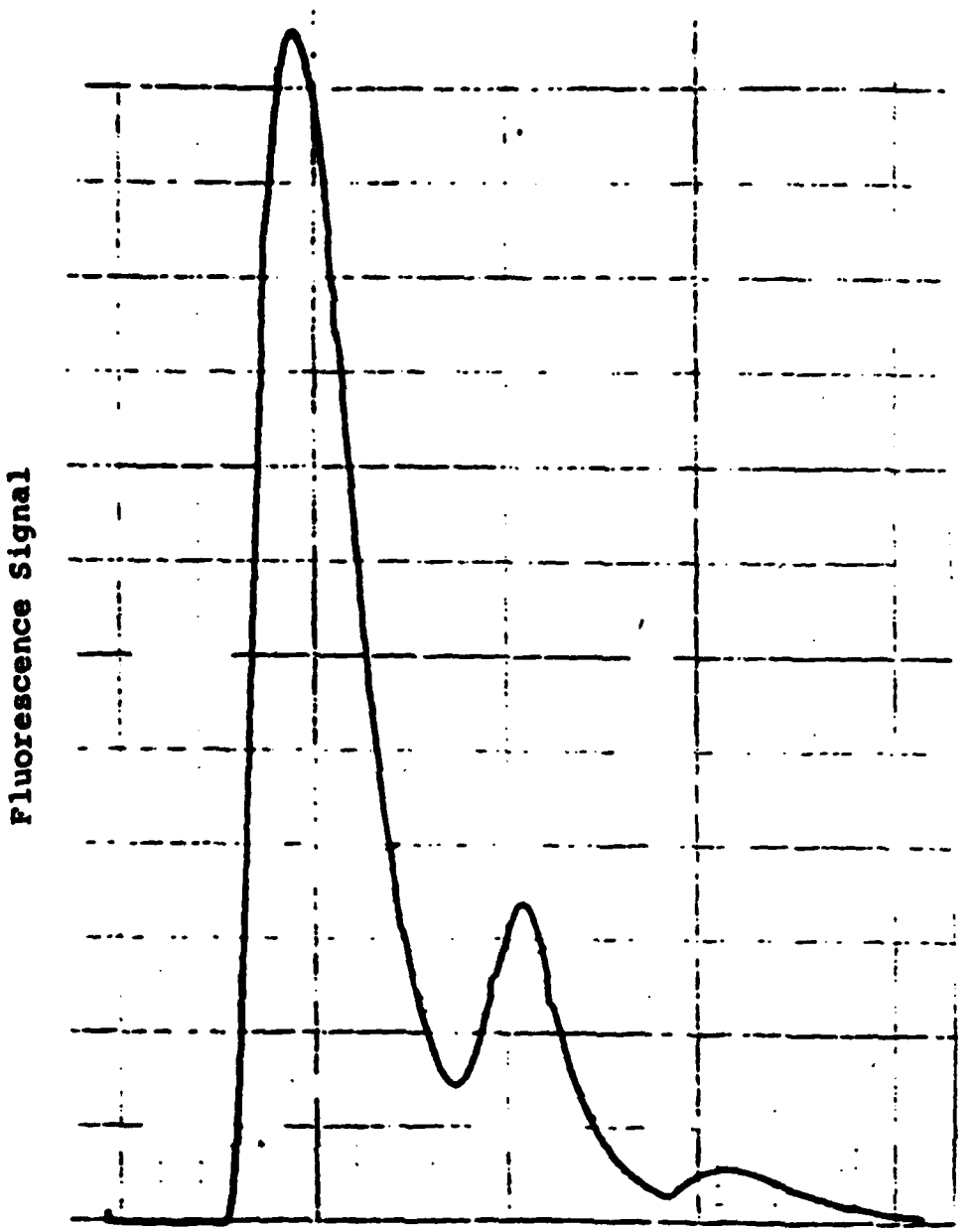

Fig. 6 - Temperature-time histogram for the desorption of iodine from silver zeolite adsorber bed. Four hundred micrograms of I_2 in one liter of air was deposited on the adsorbant. Iodine is thermally desorbed. Desorption begins at about 650°C and falls to near zero at about 975°C. See the text for a discussion of the complicating details involved in the desorption step.

iodine adsorbed on silver mordenite. Desorption does not begin until the adsorbent reaches the melting point temperature of AgI. Desorption does not end until the zeolite structure has completely collapsed and the adsorbent has melted. The color of the melted zeolite indicates that a part of the iodine remains in the melt and is not quantitatively desorbed. The heating of the zeolite generates a large amount of aerosols, likely vaporized AgI based upon color. The AgI partially decomposes in the desorption oven. However, the pyrolysis is incomplete leaving behind large amounts of solid AgI in the flow tubes and the fluorescence sample cell. This technique is unsuitable for desorbing iodine from the silver zeolites.

2.6.2.2 Sodium Zeolite

A sample of zeolite in the sodium salt form supplied by Dr. Tom Thomas of INEL was tested in the instrument. The intention of these experiments was to use the sodium zeolite as a physical rather than a chemical adsorber. We could not detect any evolution of iodine in the scrubbing cycle after deposit of iodine, probably because the iodine is chemically bound in the form of NaI. This material is unsatisfactory for use with the detector.

2.6.3 Chemical Desorption From Zeolites to Produce I_2

Dr. L. L. Burger at Battelle Pacific Northwest Laboratories[7] has shown that iodine can be stripped from silver zeolites with hydrogen gas. The hydrogen converts the AgI in the zeolite matrix to HI which is volatilized from the matrix regenerating the zeolite in the silver form. Since HI cannot be detected by the prototype iodine detector it must be reconverted to molecular iodine. In the gas phase an equilibrium exists

between the compounds;

$$2HI \underset{k_{-2}}{\overset{k_2}{\rightleftharpoons}} H_2 + I_2$$

Higher temperature favors the $H_2 + I_2$ products. For example see Table I. Unfortunately, the homogeneous gas phase kinetic rates predict a very slow approach to equilibrium. For instance, for HI at $781^{o}K$, the homogeneous reaction rate is expected to produce 1% conversion to $H_2 + I_2$ in 10^6 sec. Elevated temperature and catalysis can significantly enhance the approach to equilibrium.

Table I

$H_2 + I_2$ Equilibrium Data

$T^{o}K$	k_{-2}/k_2
556	63.2
575	52.8
629	41.7
666	32.2
700	27.7
781	17.0

We have studied the conversion of HI to $I_2 + H_2$ using the quartz catalyst oven shown in Figure 3 which is used for CH_3I pyrolysis. Mixtures of HI in helium are flowed through the catalytic oven to the iodine detector to determine I_2 concentrations. The lower curve in Figure 7 shows the I_2 fluorescence signal as a function of temperature for a 30 ml/min flow of 1/1500 HI/He mixture using the quartz catalysis tube. In different experiments the conversion efficiency was measured as a function of flow rate through the quartz catalytic oven. These measure-

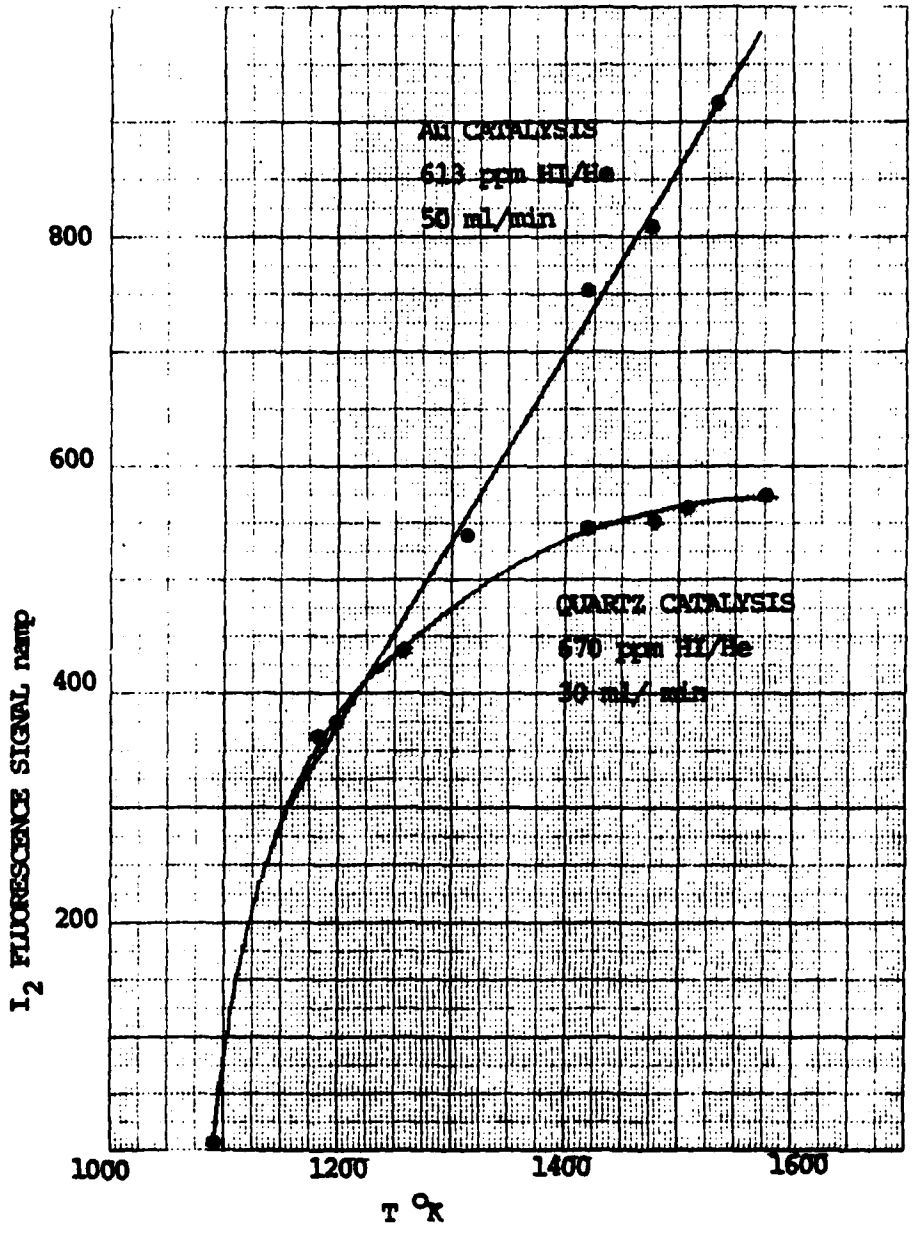

Fig. 7 - Fluorescence signals from I_2 after catalytic conversion of HI as a function of temperature. The lower curve shows data for a concentration of 670 ppm HI in He at a flow rate of 30 ml/min using only the quartz tube of the oven as a catalytic surface. The upper curve shows data for 613 ppm HI in He at a flow rate of 50 ml/min when gold foil is inserted into the tube as a catalytic surface.

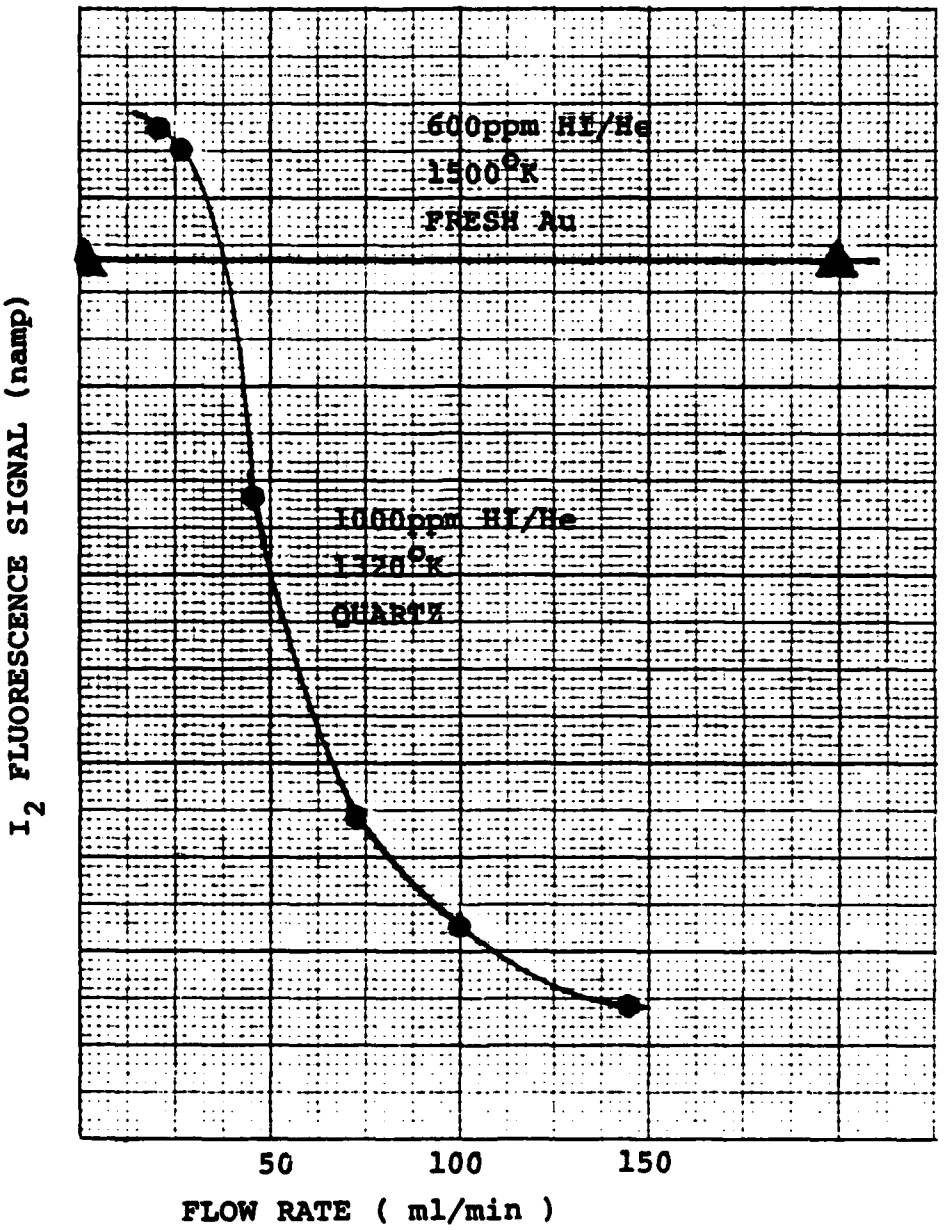

Fig. 8 - Fluorescence signals from I_2 after catalytic conversion of HI as a function of flow rate. The full circles correspond to data taken for 1000 ppm HI in He at 1320K using only the quartz tube as a catalytic surface. Solid triangles correspond to data taken for 600 ppm HI in He at 1500K when fresh gold foil is used as a catalytic surface.

ments made for a 1/1000 HI/H_2 mixture are plotted as filled circles in Figure 8 for flow rates up to 150 ml/min.

The measurements with the quartz catalyst show that we can obtain a conversion of HI to I_2 in excess of 20% at 1950°F. However, the conversion time required in the oven is in excess of five seconds. The hot quartz catalyst converts the HI with marginal efficiency, however, its catalytic activity is variable from day to day and is not dependable enough for reliable operation.

2.6.4 Use of Metallic Catalysts

A search has been made for a more efficient catalyst. There is a limited amount of data available in the literature which is relevant to this catalytically assisted reaction. These studies indicate that metallic gold is the most efficient catalyst for the conversion. The rates from these old measurements are of dubious value, however, the ranking of catalytic materials relative to each other is likely meaningful.

The quartz catalyst tube was packed with metallic gold and an HI/He mixture (1/1630) was flowed through the catalyst. The molecular iodine product was detected with the Bendix detector. The upper curve in Figure 7 shows the conversion efficiency to molecular iodine as a function of temperature.

At 2100°F the conversion efficiency remains constant for flow rates up to 200 ml/min and scales linearly with HI feed gas concentration over a range of 50 in concentration. This insensitivity to flow rate is shown in the Figure 8 plot for the filled triangles. Unfortunately, the gold catalyst appears to pcison after about two hours of operation and the efficiency is reduced to that obtained with the quartz tube alone.

Currently, experiments are being carried out to determine methods of catalyst preparation which are more resistant to poisoning and reduction in efficiency.

2.7 SUMMARY AND FUTURE WORK

The prototype Iodine (129) detector from Bendix was quality assurance tested and accepted. It performed at the design specification of 10^{-10} g/cm^3 for I (129). Evaluation of NO_2 interference levels showed that NO_2 at the 3000 ppm level represents an interference for I (129) concentration measurements at iodine concentrations less than $\sim$3 ng/cm^3. Because of the sensitivity limitations and because of the NO_2 effluent levels present, the Bendix prototype cannot be field tested at INEL for real time flowing gas samples at available test stations. Upon recommendation of DoE, NRL during early FY80 will investigate the feasibility of field operation of the detector in a real time mode at an appropriate test site at the Savannah River Facility.

Techniques are being developed to increase the sensitivity of the prototype iodine detector by batch processing which will also allow a discrimination against NO_2 interferences. Charcoal scrubbers have been shown to be efficient for batch processing of I_2 and organic iodides. Detection limits for I_2 can be extended to any desired limit by extended scrubbing of the sample airstreams. Unfortunately, the charcoal adsorbent cannot be used to discriminate against airborne NO_2.

Silver zeolites are shown to scrub I_2 and converted organic iodides. Thermal desorption cannot be accomplished without destruction of the zeolite matrix. Thermal stripping produces aerosols of AgI which render

the technique impractical. H_2 gas can be used to strip I_2 from the zeolite beds as HI. Various catalytic techniques have been investigated to convert HI to I_2 for detection in the prototype detector. Gold works well but appears to poison after short periods of operation.

Current evaluation indicates that vaporized silica is responsible for the poisoning. Experiments will be carried out in FY80 to verify this and other carriers for the Au catalyst will be evaluated for use in the catalytic oven.

In addition measurements will be made to determine if iodine can be stripped from the loaded zeolite by chemical desorption with methane to produce methyliodide. This material is more compatible with our current batch processing capabilities than is HI.

It is hoped by the end of FY80 to completely specify and demonstrate the I (129) detector operation in a batch processing mode.

2.8 REFERENCES

1. "Environmental Aspects of Nuclear Power"
   G. G. Eicholz
   Ann Arbor Science, Inc., 1976.
2. "Control of Iodine in the Nuclear Industry"
   Technical Reports, Series No. 148 (Vienna: International Atomic Energy Agency, 1973).
3. "Environmental Radiation Dose Commitment: An Application to the Nuclear Power Industry"
   Report EPA-520/4-73-002, U. S. Environmental Protection Agency, Washington, D. C., 1974.

4. "A Radioiodine Detector Based on Laser Induced Fluorescence"

A. P. Baronavski and J. R. McDonald

NRL Memorandum Report 3514, Naval Research Laboratory, May 1977.

5. "A Radioiodine Detector Based on Laser Induced Fluorescence"

A. P. Baronavski and J. R. MCdonald

Proceedings of the 15th DoE Nuclear Air Cleaning Conference, Boston, MA, 7-10 August 1978, published February 1979.

6. "Detection and Monitoring of Airborne Nuclear Waste Materials - Annual Report to the Department of Energy"

J. R. McDonald, A. P. Baronavski, L. R. Pasternack-Rafferty, V. M. Donnelly, and R. C. Clark

NRL Memorandum Report 3895, December 1978.

7. Nuclear Waste Management Quarterly Progress Report

Pacific Northwest Laboratories, Richland, Washington

Project Manager, L. L. Burger.

SECTION III

AN OPTICAL DETECTOR FOR TRITIUM

3.1 INTRODUCTION

Tritium is produced by numerous mechanisms associated with various operational components of nuclear reactors. Its production is indigenous to these operations and represents an increasing problem both to the nuclear industry and in fuel handling and reprocessing operations. Chemically the isotope exists in the gas phase primarily as HTO and HT with some contribution from tritiated hydrocarbons. The relative importance of these species depends on the production and handling environment of the isotope.

The maximum permissible concentration of tritium in air in the chemical form of HTO is 2×10^{-7} $\mu C/cm^3$. However, because the radioactive decay is weak (β = 18 Kev), it is one of the most difficult nuclides to measure in real time.[1]

3.1.1 Detection Techniques

Currently existing detection methods make use of various radiocounting techniques such as ionization chambers,[3,4] liquid scintillation[5,6] counting, solid scintillators,[1] and proportional counters.[7,8] Each of these detection techniques suffer from unique limitations, however, they have in common a potential interference problem from other nuclides such as ^{85}Kr and ^{14}C. In addition, a sensitivity to gamma radiation poses a problem in detection.

Because of the interference problems and because the tritium exists in a variety of molecular forms, detection schemes must make use of catalytic converters to produce a single molecular isotope and separators

to remove the tritium from large volumes of air containing the interfering nuclides.[2] The separators typically make use of either silica gel or molecular sieves for trapping of the aqueous component. This operation reduces the detector to operating in a non-real time batch mode. The most novel separator under investigation makes use of a technique referred to as permeation distillation.[2,9,10] In this application the tritiated water is continuously removed from the airstream in a gaseous counter current extraction. This technique is amenable to continuous monitoring applications and gives an adequate separation from ^{85}Kr and high levels of NO_2.

3.2 OPTICAL DETECTOR EVALUATION

Under contract with DoE in FY79, we have been investigating the use of an optical detector for tritium which circumvents the problems of interference encountered in radio-counting methods of detection. The technique used is the measurement of emission intensity from the Balmer-α line of hydrogen and has been described previously.[11]

3.2.1 Optimizing the Tritium Signal

Measurements were performed to determine the dependence of hydrogen Balmer-alpha (H_α) and deuterium Balmer-alpha (D_α) signal levels on lamp current, water vapor (and gaseous H_2) flow rates, carrier gas flow rates, and total pressure. The apparatus used in these measurements is shown in Figure 9. Basically, it consists of a low pressure (1-100 torr) flow of carrier gas into which is injected a small (0.1 to 10%) flow of H_2O, D_2O, or H_2. The gases mix, flow through an electric discharge lamp, and are pumped away. Alternately, the lamp may be run in the sealed-off, non-flowing mode. The discharge lamp consists of a

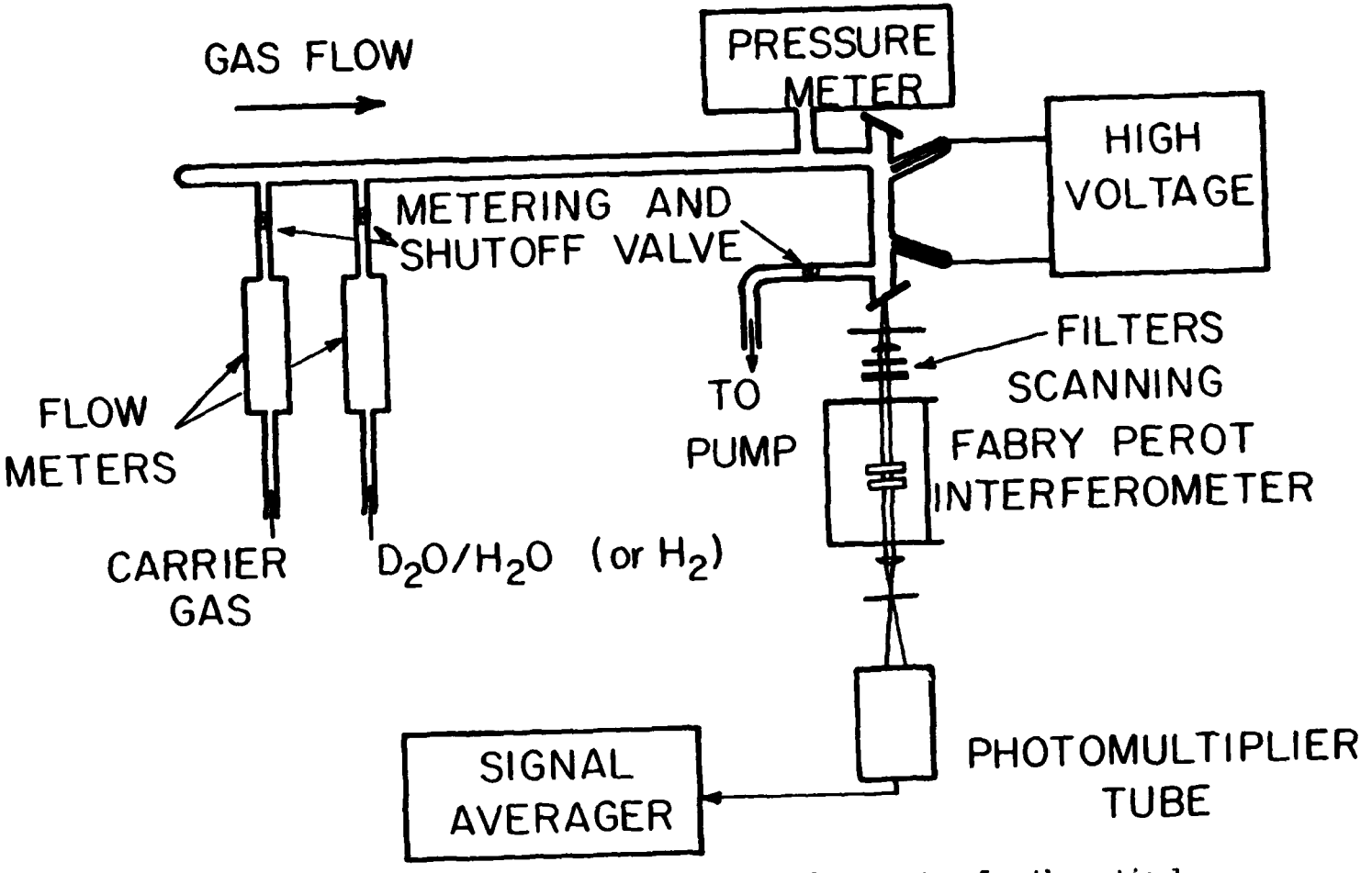

Fig. 9 - Block diagram of the experimental apparatus for the optical tritium detector. See text for details.

2 mm O.D. capillary tube with entrance and exit ports for gas flows and tungsten electrodes sealed to the tube. The small bore tubing is necessary to obtain maximum throughput of the emission into the detector.

A scanning Fabry-Perot interferometer (or initially an 0.6 m monochromator) is used to spectrally isolate the H_α and D_α emission lines at 656.5 and 656.3 nm, respectively. Spectral scans can be displayed on a strip chart recorder or summed on a signal averager to improve the signal-to-noise ratio (S/N).

The H_α signal intensity as a function of H_2O flow rate is shown in Figure 10 for three helium carrier gas pressures. The H_α signal was found to maximize at H_2O flow rates of 10 to 30 standard-cubic-centimeters-per-minute (std. cc/min, or SCC/M). The H_α signal was also measured as a function of total (He) pressure. Typical data is shown in Figure 11 for two different H_2O flow rates. The signal maximizes at a total pressure of about 10 torr. The same measurements were carried out for H_2/He mixtures. The optimum operating conditions for both H_2O and H_2 in He are given in Table II.

Table II

Optimum Conditions for Operating the Discharge Flow Lamp

H_2O or H_2 Flow	He Flow	Total Pressure	H_α Relative Signal
H_2O: 20±10 scc/m	1000±500 scc/m	10±5 torr	1.0
H_2: 25±10 scc/m	1400±500 scc/m	14±5 torr	1.4

Within experimental uncertainty, the concentrations and total pressures necessary for optimum signal are the same under non-flowing conditions. However, signal stability is somewhat of a problem with a static gas

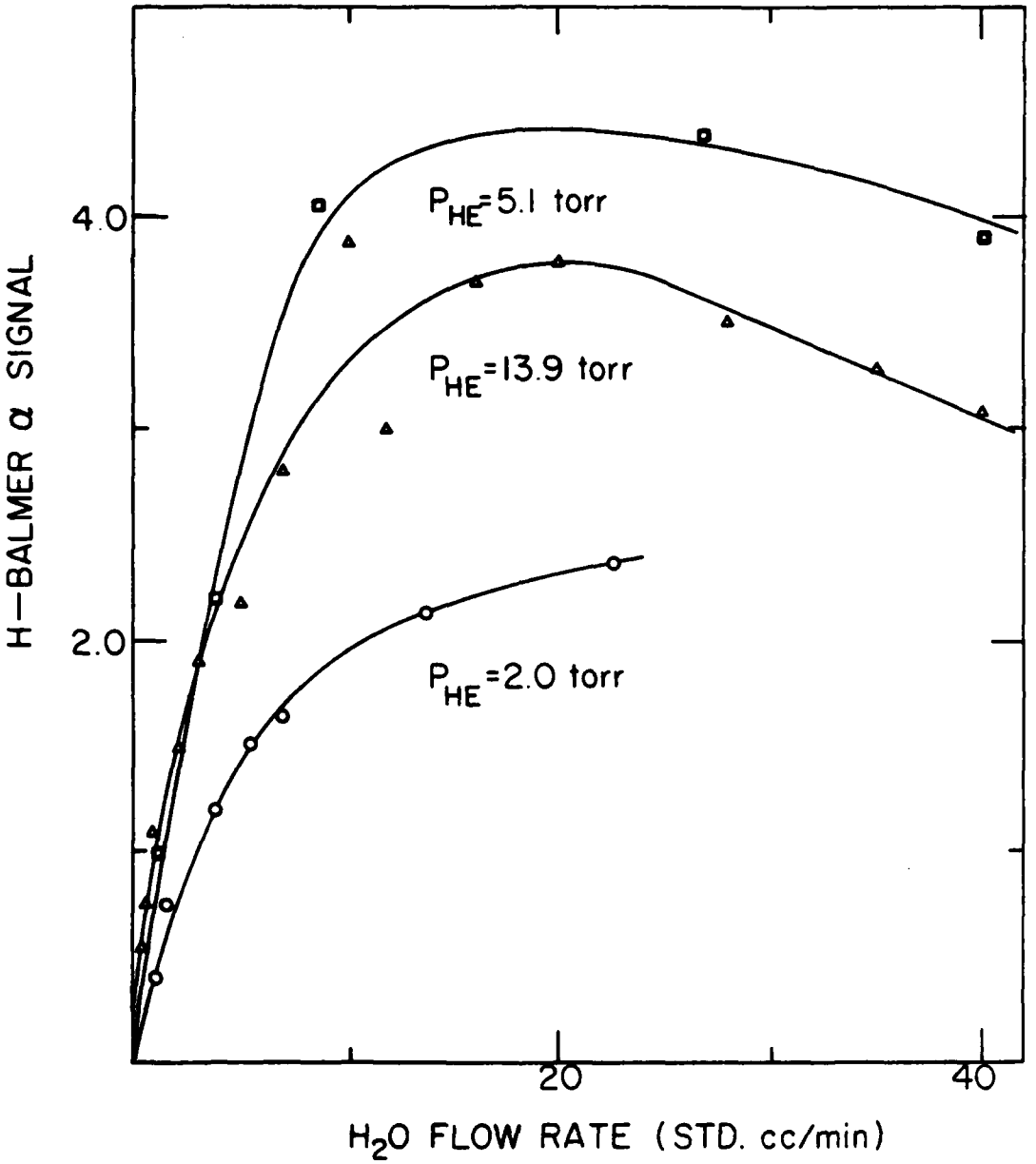

Fig. 10 - Hydrogen Balmer-α signal intensity as a function of H_2O flow rate. Data are shown for three pressures of He.

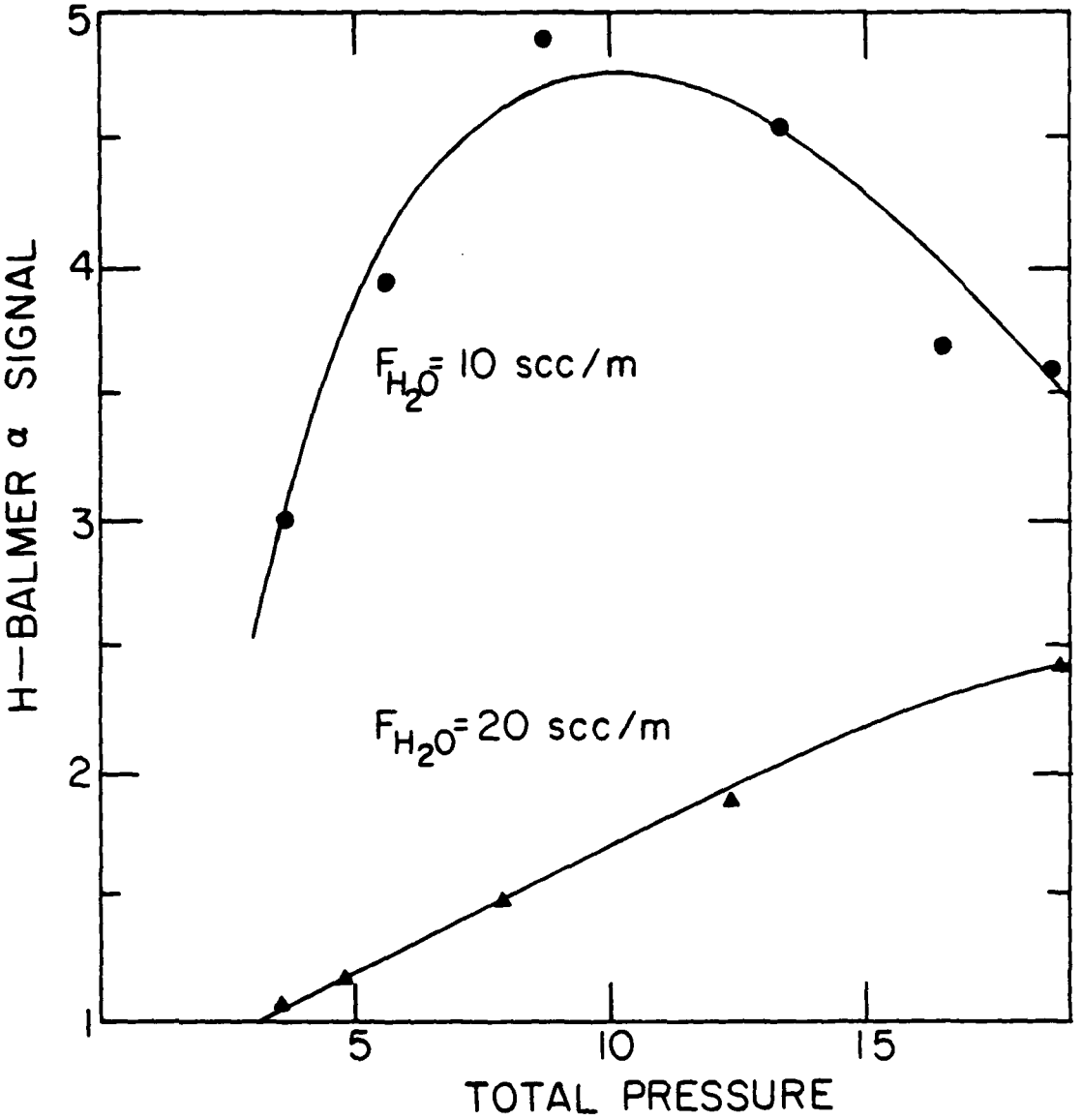

Fig. 11 - Hydrogen Balmer-α signal intensity as a function of total pressure. Data for two flow rates of H_2O are shown. The intensity for the F = 20 scc/min rate at its peak would be lower than that for F = 10 scc/min by ∿ a factor of 2.

fill, due to water adsorption into or desorption from the vacuum system. Consequently, all subsequent measurements were done under flowing conditions.

In order to obtain [T], the absolute tritium concentration, it is important that the ratio $[T]/T_\alpha$ be a constant, independent of [H] and [D] levels, but dependent only on the total [T]+[D]+[H] concentration. We expect that to a close approximation,

$$[H]/H_\alpha \tilde{=} [D]/D_\alpha \tilde{=} [T]/T_\alpha.$$

To test the validity of this approximation, known $[D_2O]/[H_2O]$ mixtures were run under the conditions given in Table II. The results are shown in Table III. Within experimental errors the ratio of $[D_2O]/[H_2O]$ is identical to the D_α/H_α signal ratio, as expected, meaning one always has an internal standard (i.e., hydrogen or deuterium signal) upon which to scale the tritium signal.

Table III

D_α/H_α Signal Ratio as a Function of $[D_2O]/[H_2O]$ Concentration

Water Flow = 15 scc/m, Total Pressure = 10 torr (He Carrier)

$[D_2O]/[H_2O]$	D_α/H_α
1.00	0.85
0.11	0.19
0.020	0.016
0.010	0.012
0.00015	0.0002

3.2.2 Fabry-Perot Interferometer

The main component of the optical tritium detection is a scanning Fabry-Perot interferometer. The basic principles of interferometry have been discussed in a previous report.[11] An interferometer is

essentially a high (i.e., 90%) throughput, high resolution (up to 10^{-3} cm^{-1}) spectrometer. These two features are essential for detection of low T_α signals in the presence of large H_α and D_α signals.

The free spectral range (FSR) of an interferometer is defined as the spectral region which can be covered without overlapping the next order of transmission. As stated previously, the optimum FSR for the tritium detector is about 12 cm^{-1}, roughly twice the spacing of the H_α and T_α signals. The FSR is related to d, the plate separation by

$$FSR = 1/2d$$

The plate separation was set to approximately 0.04 cm. The FSR was then accurately determined by measuring the separation between H_α and D_α lines. The FSR was found to be 14.63 cm^{-1}.

The finesse (F) of an interferometer is defined as

$$F = FSR/(resolution)$$

The theoretical finesse attainable with a single-pass interferometer is given by

$$\frac{1}{F_l^2} = \frac{1}{F_r^2} + \frac{1}{F_f^2} + \frac{1}{F_i^2}$$

where $F_r = \frac{\pi (R)^{\frac{1}{2}}}{1-R}$ is the reflectivity finesse for plates with reflectivity R at wavelength λ, $F_f = \frac{M}{2}$ is the flatness finesse for λ/M flatness, and $F_i = \frac{4\lambda L^2}{D^2 d}$ is the instrument finesse for an aperature of diameter D located a distance L from the plates and d is the plate separation. For our instrument, the theoretical finesse $F_l = 35$. This was found to compare favorably with an actual finesse of 20 observed by scanning over the output of a He-He laser, indicating that the instrument was performing properly in the single-pass mode.

The scattered light rejection and finesse are greatly enhanced by running the interferometer in a multipass mode. The multipass finesse is given by

$$F_p = \frac{F_1}{(2^{1/p} - 1)^{1/2}}$$

where p is the number of passes. For three passes, the theoretical finesse is therefore 68, while the actual observed finesse with our instrument was found to be 50. The agreement between the observed and calculated three pass finesse can be considered quite good.

The scattered light rejection measured at one half the FSR is known as the contrast. The contrast is given by

$$C_p = \left[\frac{4F_1^2}{\pi^2}\right]^p$$

for three passes with a theoretical finesse of 35, $C_p = 1.2 \times 10^8$, compared to an actual value of $\sim 10^7$. A contrast of 10^7 is more than adequate.

In summary, the interferometer appears to possess the anticipated properties necessary for detecting low tritium levels.

3.2.3 Techniques for Water Separation

The proposed method for detecting tritium involves the removal of water from the input gas stream, as shown in Figure 12. We have carried out tests to evaluate the feasibility of using an "on-line" permeation-distillation tube to accomplish this task (see Figure 13). The input airstream enters the product input side of the distillation tube. The water wets the membrane, permeates through the membrane, and is removed on the other side by a dry carrier gas. The carrier gas then flows through the discharge lamp. Tritiated water must be separated from the

TRITIUM DETECTION

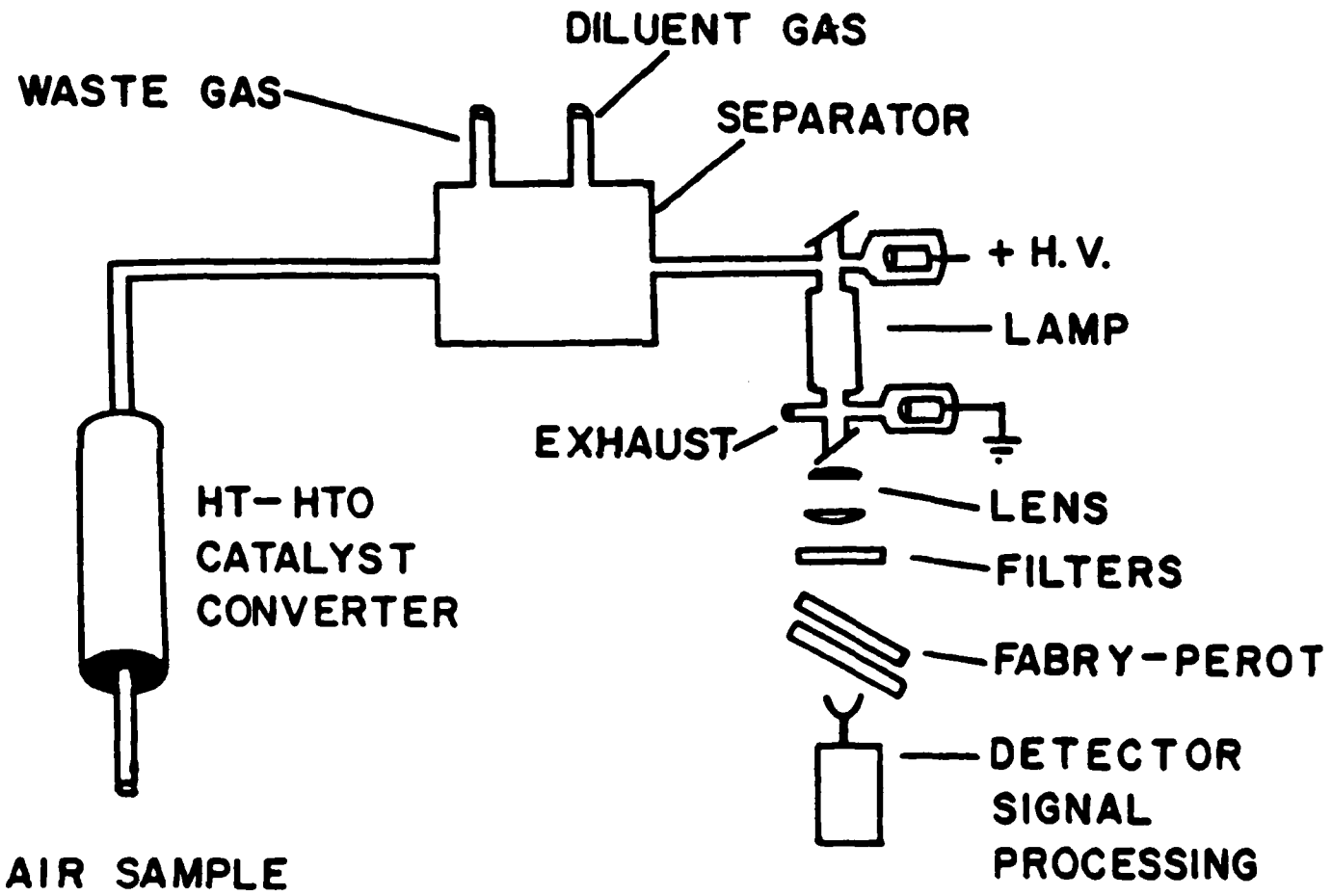

Fig. 12 - Schematic diagram of the breadboard tritium detector. The detector consists of four major components: the HT → HTO catalyst unit, the HTO gas separator, the discharge lamp, and the detection-signal processing component.

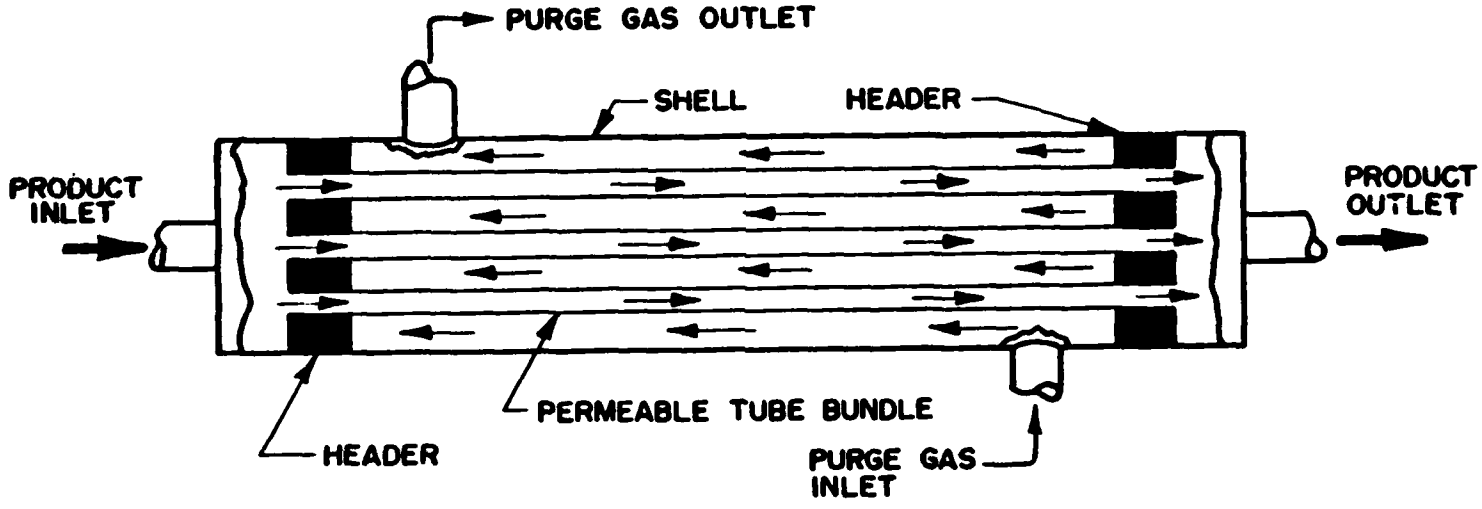

Fig. 13 - Permeation distillation tube used to separate water vapor from airstreams. The water vapor exits the tube with the carrier gas at the purge gas outlet. (See also Figure 12).

input air sample because species such as N_2 and NO_2 interfere with optical detection of tritium. This interference will be discussed in more detail in the next section.

Air saturated with H_2O was introduced into the product inlet and He used to dry the membrane and carry the H_2O into the discharge lamp. The H_α signal from discharge increased to a stable signal in one hour. The product inlet was then rapidly switched to air bubbled through a 50/50 mixture of D_2O/H_2O, and D_α/H_α signal ratios measured as a function of time. The rise in the D_α/H_α ratio is shown in Figure 14. After five hours of continuous injection of equal ratios of D_2O and H_2O at the product inlet side, the D_2O/H_2O ratio on the output side is still only 0.25. Indications are that it would take at least another 5 to 10 hours to achieve the proper ratio of 1. When the output ratio reached 0.25, the input air was switched back to natural abundance H_2O. The D_2O/H_2O output ratio remained essentially constant at 0.25 for nine hours, before finally starting to decrease. The decrease was exponential with time, as shown in Figure 15, with a decay time of 0.83 hours. The transport time of water through the membrane was found to be only slightly dependent on air and He flows, and temperature between 25 and 120°C.

It is our conclusion that the distillation separator cannot be used if one wants to monitor changes in tritium concentrations over a period of minutes. In these instances, a cryotrap, dessicant, or sieve trap is the preferred method of capturing water from the input airstream. However, for long term (∿24 hour) monitoring of tritium, the distillation tube can be used.

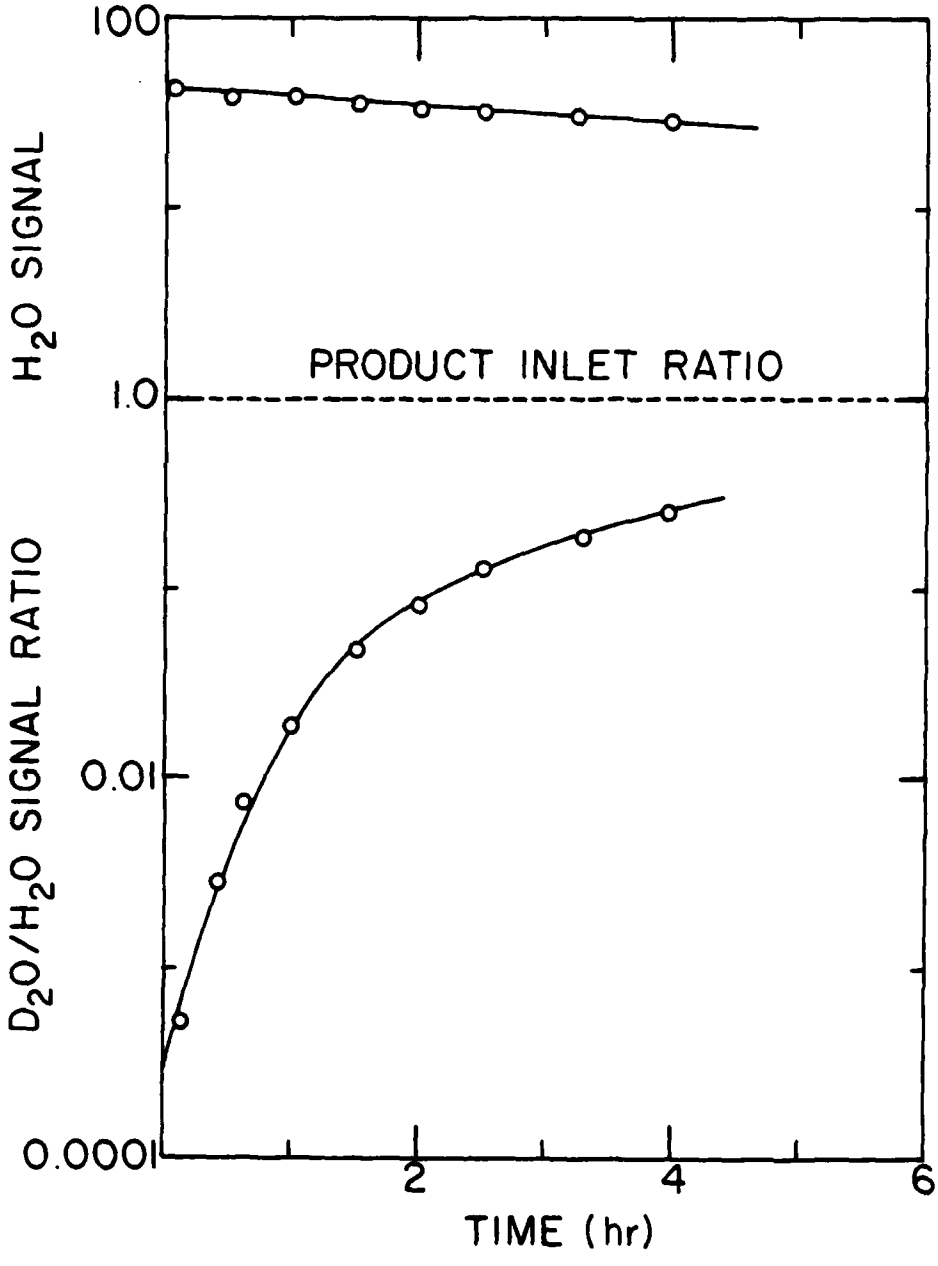

Fig. 14 - D_2O/H_2O signal ratio as a function of time for a 1 to 1 D_2O/H_2O concentration ratio. The upper panel shows the decrease in absolute H_2O signal due to replacement of ambient H_2O on the tube by D_2O. The lower panel shows the asymptotic approach of the measured signal to the signal expected from the product inlet ratio.

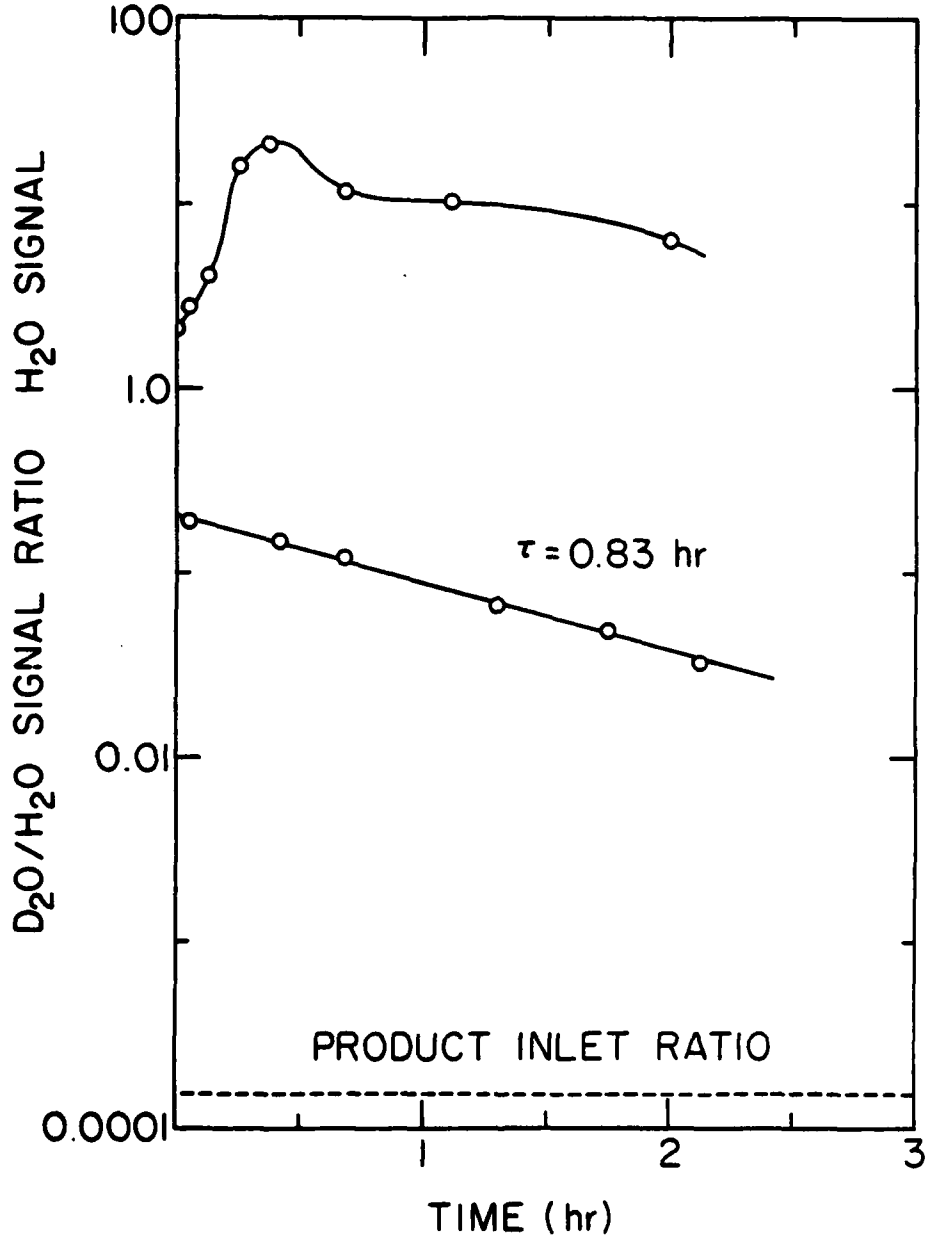

Fig. 15 - D_2O/H_2O signal ratio as a function of time for natural abundance D_2O in H_2O. This shows the characteristic response time of the permeation tube to changes in the inlet ratio, γ = 0.83 hours.

3.2.4 Detection Sensitivity

The apparatus shown in Figure 9 was used to evaluate the absolute sensitivity for tritium in the form of HTO. The lamp was run using a 1% D_2O in H_2O flow in He carrier, with the optimum flow rates and pressure given in Table II. A sample interferometer spectrum of the lamp output is shown in Figure 16 for He carrier gas. In Figure 16, H_α signal has been allowed to run approximately 30X off scale. The D_α peaks are clearly seen in this scan. The valley between the D_α peak and the next order of the H_α peak is shown expanded X64. The wavelength at which the T_α peak would be found (tritium is not present in the discharge lamp) is also shown in Figure 16. The background (X64) was recorded with the lamp output blocked and is due mostly to the photomultiplier tube dark current of about 20 counts/sec. The spectrum shown in Figure 16 was averaged over 8192 scans. The interferometer scans over this spectral region at a rate of 10 scans/sec for a total accumulation time of 13.6 min. The signal averager digitizes the sweep into 10^{-4} sec intervals. Under these conditions, the H_α and D_α signals are 1.7×10^6 and 5.6×10^4 counts/channel. The background level (B) at T_α is B = 470 counts/channel.

From the signal levels in Figure 16, one can calculate the ultimate tritium sensitivity. Since the spectrum is repetitively scanned over many scans, noise caused by lamp instability, high voltage power supply ripple, etc., becomes negligible. The only source of noise under these circumstances is statistical noise inherent in the measurement. For a signal level of Y counts, the single standard deviation uncertainty is given by $\pm (Y)^{\frac{1}{2}}$. Consequently, in the spectrum shown in Figure 16, the noise level N integrated over the T_α band width at T_α line center is

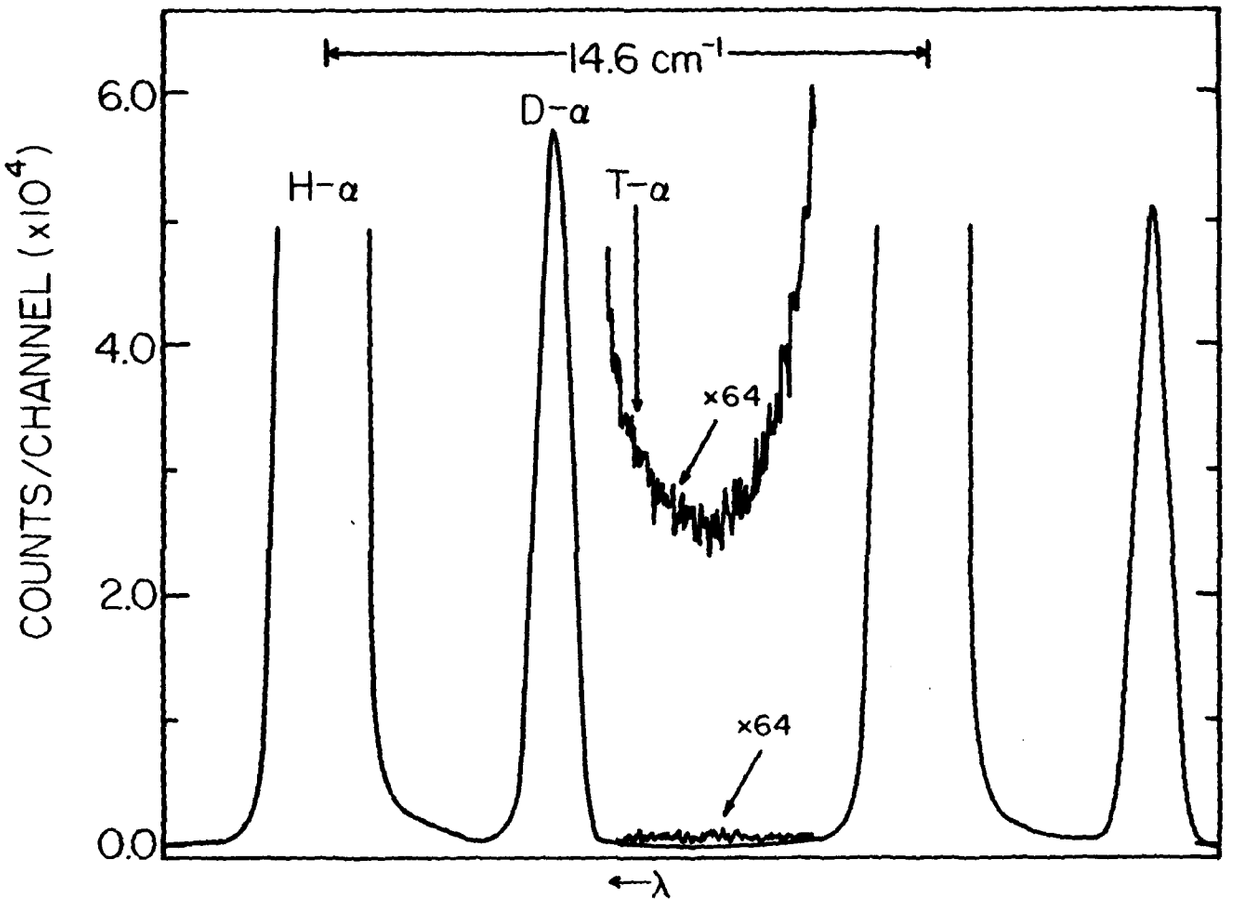

Fig. 16 - Interferometer spectrum of discharge lamp output. In this spectrum the deuterium concentration is 1% of the hydrogen concentration. The lower trace is expanded by 64 times with the lamp blocked to show the "dark counts" of the system. The upper trace is also expanded by 64 times with the lamp unblocked and gives a measure of the background emission in the region of the tritium-α line.

$N = (B)^{\frac{1}{2}} = (470)^{\frac{1}{2}} = 22$ counts/channel. So, for a signal-to-noise ratio (S/N) of 1, $T_\alpha = 22$. This means that for the conditions used to record the data in Figure 16, one could detect a T_α signal level 7.7×10^4 smaller than the H_α signal level. The interference filters used to isolate the 656 nm spectral region pass T_α emission four times as efficiently as H_α radiation, so we were actually at the level of being able to detect one T-atom for every 3.1×10^5 H-atoms in the discharge.

One major improvement which can be easily realized is to increase the transmission of the interference filters. The 656 nm filter transmits about 30% at T_{max}. This could be increased by a factor of two with a commercially available filter. A second filter was found necessary to block some unidentified long-wavelength emission which "leaked" through the 656 nm filter and contributed to a large background. This second filter (T_{max} = 650 nm) has a transmission at 656 nm of only about 10%. This will therefore be improved by a factor of 6, with choice of the proper filter, for an overall increase (both filters) of about a factor of about 12. This increases the sensitivity to one T-atom in 1.1×10^6 H-atoms in the discharge.

For the optimum conditions given in Table II, the total water concentration is 2% water in He. At a total pressure of 10 torr this corresponds to a water concentration of 6×10^{15} cm^{-3} or a tritium sensitivity of 6×10^9 cm^{-3}, <u>in the discharge lamp</u>.

The ultimate sensitivity to tritium, present as HTO, in air can now be evaluated. This sensitivity will depend on the total water content of the air sample. Assuming a partial pressure of 24 torr water (7.4×10^{17} molecules/cm^3), corresponding to 100% humidity at 25°C, the

HTO sensitivity is 6.8 x 10^{11} HTO molecules/cm^3, or 2.7 x 10^{-2} $\mu C/cm^3$. Further improvements can be made in the optical tritium detector by the techniques indicated to lower the sensitivity limits. Two independent developments during the past year have led us to reconsider:

a. Workers at INEL[2] have developed a tritium technique capable of monitoring the MPC level with a hold-up time of ∿24 hours;

b. It now seems probable that the scanning diode spectrometer to be described in Section IV can be adapted to also measure tritium in a near real-time mode.

For these reasons we propose to suspend development of the optical detector while we investigate the technique described in Section 3.3.

3.3 RECOMMENDATIONS AND FUTURE PLANS

In Section IV, it is shown that long path length infrared absorption is a very sensitive technique for monitoring gas phase species. We propose that this technique be investigated as a real time (on the order of a few minutes) monitor for HTO. The equipment to be used is identical to that described in Section IV with the addition of another laser diode to reach the region of the spectrum where HTO absorbs strongly. Although little is known about HTO spectroscopy, this information can be obtained by using such techniques as Fourier Transform IR absorption. We are presently negotiating with personnel at LASL concerning the possibility of obtaining spectra of HTO with their instrument.

An advantage that this method would have is that one instrument could be used to obtain both $^{14}CO_2$ concentrations and HTO concentrations, with only a change in diodes. The holder in our spectrometer will

accommodate up to four diodes in the cryostat. Of course, much depends upon the ability to find regions of HTO absorption where interferences from other species are negligible. This question can only be answered after spectra of HTO have been obtained and analyzed with respect to other species which are present in the off gas.

3.4 REFERENCES

1. National Council on Radiation Protection and Measurements, Tritium Measurement Techniques
   NCRP Report No. 47 (1976).
2. "Development of a Continuous Tritium Monitor for Fuel Reprocessing and Waste Solidification Facilities"
   S. J. Fernandez and G. D. Pierce, presented at the 34th Northwest Regional American Chemical Society Meeting, Richland, Washington, June, 1979.
3. "A Single Instrument for the Determination of Tritium in Mixtures of Hydrogen Isotopes"
   I. Lewkowicz and M. Rosmann
   Nucl. Instrum. Methods 126, 149 (1975).
4. "A Portable Monitor for Tritium in Air"
   R. V. Osborne and A. S. Coveart
   Nucl. Instrum. Methods 106, 181 (1973).
5. "Monitoring Reactor Effluents for Tritium: Problems and Possibilities"
   R. V. Osborne
   Tritium, A. A. Moghissi and M. W. Carter, eds., Messenger Graphics, p. 496 (1970).

6. "Continuous Monitoring of Aqueous Tritium Activity"

P. Ting and R. L. Little

Tritium, A. A. Moghissi and M. W. Carter, eds., Messenger Graphics, p. 170 (1970).

7. "Tritium Survey Instruments"

G. E. Driver

Rev. Sci. Instrum. 27, 300 (1956).

8. "Proportional Flow Counters for Measurement of Tritium in Air"

R. Ehret

Assessment of Airborne Radioactivity, International Atomic Energy Agency, p. 531 (1967).

9. "Evaluation of the HEPA Filter In-Place Test Method in a Corrosive Off-Gas Environment"

L. P. Murphy, M. A. Wong, and R. C. Girton

15th DoE Nuclear Air Cleaning Conference, Boston, MA, August 1978.

10. "Continuous Drying of Process Sample Streams Perma Pure Products, Inc., Manufacturer's Literature, Oceanport, NJ, 1973.

11. J. R. McDonald, A. P. Baronavski, L. R. Pasternack-Rafferty, V. M. Donnelly, and R. C. Clark

NRL Memorandum Report 3895 (1978).

SECTION IV

AN OPTICAL $^{14}CO_2$ DETECTOR

4.1 INTRODUCTION

4.1.1 Production Sources and Production and Release Levels World-Wide

With the continued world-wide growth of the nuclear industry there is a valid increasing concern as to the global impact associated with the discharge of the long-lived radio-nuclides. One of the most significant of these is Carbon 14. A concerted effort is being devoted to evaluate release limits, to control production, and to the development of cleanup techniques for this isotope. Various monitoring and measurement techniques are currently under development. Table IV, based on data derived by Davis,[1] shows an evaluation of the production sources and levels associated with various power reactors.

TABLE IV

PRODUCTION RATES OF ^{14}C IN SEVERAL REACTOR TYPES

	Carbon 14 Production Rates $Ci/GW_{(e)}$ Yr.			
Reactor	Coolant	Fuel	Moderator and Annulus System	Cladding and Structural Matter
BWR	4.7	17.6	-	43-60
PWR	5.0	18.8	-	30-42
LMFBR	-	6.3	-	12.8
ATGR	-	12	-	<190
Candu-540 MW	9	15	870	-
Candu-750 MW	10	20	547	-

The Carbon 14 from these reactor sources exists as a variety of molecular species, typically a mixture of CO_2, CO, and hydrocarbons.

The ratio of these species varies strongly with the type of reactor system. For instance, Kunz[2] reports that ^{14}C measured in PWR reactors exists mainly as hydrocarbons, while the production in BWR stations[3] is more than 90% in the form of CO_2.

Reprocessing plants represent a significant potential production source for ^{14}C also. For instance, a production is estimated in the range of 400-2200 Ci of ^{14}C per year for a LWR fuel reprocessing plant treating 1500 metric tons of heavy metal annually with a range of 40-240 ppb of $^{14}CO_2$ in a reference flow of 500 scfm of off gas.[4]

Release rates from PWR and BWR stations have been measured to be in the region of 6-8 $Ci/GW_{(e)}$ year.[2,3] In the BWR stations this release is at levels up to several hundred picocuries/cm^3 of air.[5] ^{14}C release from the HTGR reprocessing facility has been evaluated by Snider and Kaye.[6]

4.1.2 Monitoring and Control Requirements

At this point no requirements have been issued relating to the monitoring and control of Carbon 14 effluents. A large body of literature[7-9] and studies[10,11] on the environmental impact of ^{14}C are now available, and it seems evident that requirements for the control and monitoring of ^{14}C releases will be formulated in the near future.

4.1.3 Carbon-14 Monitoring Methods

A carbon-14 radioactivity level of 100 pci/cm^3 corresponds to a $^{14}CO_2$ concentration of 2.3×10^{-11} g/cm^3 or 3×10^{11} molecules/cm^3. In air this level of activity corresponds to a concentration of ~10 ppb. Therefore, any real time detection technique with practical sensitivity must have routine detection capability in the range of 1-10 ppb. At

the present time no such instrumentation exists. The only instrumentation currently available with near real time capability is conventional infrared spectroscopy. The practical detection limit for these instruments is ∿1 ppm. In addition, it is doubtful that this equipment can distinguish $^{14}CO_2$ from $^{12}CO_2$.

Several scrubbing techniques have been developed with greater sensitivity. The most sophisticated of these systems separates carbon-14 gaseous compounds with a gas chromatograph and measures them by radio counting.[9] This instrumentation is very expensive and too complex for routine use. More typically CO_2 is removed from feed streams by scrubbing with bubblers in a dissolving solvent followed by radio counting. This technique is tedious to use, subject to contamination by other radioactive species and has not yet proven effective at below the ppm range.[9]

The most reliable instrumentation for use at the sub ppm range currently involves use of a fractionating column with nickel catalyst to convert carbon species to CH_4 followed by separation by gas chromatography with subsequent analysis by flame ionization detection.[9] This instrumentation has been used to measure carbon-14 at the 100 ppb level with an uncertainty of a factor of two.

It is apparent that none of the presently available analytical instrumentation is suitable for real time measurement of $^{14}CO_2$. Even the best techniques have a sensitivity limit near 100 ppb. The instrumentation is extremely sophisticated, quite expensive, and is unlikely to be applicable for routine use for widespread effluent analysis.

4.2 OPTICAL CARBON (14) DIAGNOSTIC EVALUATION

The interagency contract between DoE and NRL was modified at mid-year FY78 to allow for a feasibility study of new detection techniques which might be applicable for $^{14}CO_2$ monitoring in the effluents of nuclear facilities. It was assumed that a 1-10 ppb sensitivity range is required. Current techniques involving scrubbing and radio counting or gas chromatographic separation with radio counting or flame ionization detection appear to fall short of this limit even with more and more sophisticated adaptations of the instrumentation. For this reason, we chose to concentrate upon optical techniques. Vacuum ultraviolet, visible and conventional infrared techniques were rejected for a variety of reasons. Several infrared laser techniques were evaluated in detail including:

a. Tunable TEA CO_2 lasers;

b. High pressure CO lasers;

c. Optical parametric oscillators; and

d. Tunable diode lasers.

As explained in reference (12) the scanning infrared diode laser technique was recommended for development.

4.3 SCANNING INFRARED LASER DIODE SPECTROMETRY

4.3.1 Evaluation of Interferences and Choice of Frequency

In order to make analytical measurements with an ultra high resolution source such as the laser diode, several parameters must be known with high precision. These include:

a. Vibrational and rotational line positions in the accessible spectral region;

b. Similar information for all other isotopic species and possible interferents;

c. Absorption coefficients and linestrengths for resonances in the chosen spectral region.

As explained in Reference 12 much of this information is available for $^{14}C^{16}O_2$ and other carbon and oxygen isotopic species for CO_2. During FY79 further spectroscopic information has become available concerning the spectra of possible interfering gases in the CO_2 region of interest. This includes such gases as H_2O, NO, NO_2, CO, and CH_4. This information is important because it allows one to specify the spectral region to cover. The individual laser diodes will scan only over a limited frequency range (± 15 cm^{-1}). With this new information it was possible to make an informed choice of the P-branch line to monitor and thus to specify the diode for purchase.

4.3.2 Sensitivity Considerations

As pointed out in Reference 12 the calculated sensitivity for carbon (14) dioxide using long path length absorption and second derivative detection is well below the ppb range. A decision had to be made as to the correct choice of white cell to give the capability for long path measurements. A trade off is involved, the longer the path length the higher the sensitivity. However, increased path length comes at the expense of operational complexity. A decision was made to have fabricated a white cell which can be easily operated at 100 meter path length but which has a reasonable hold-up volume. The system of choice is a 1 meter, 100 pass cell with a hold-up volume of $\sim$12 liters.

4.3.3 Specification and Purchase of the Instrument

There is only one commercial vendor presently capable of supplying the instrumentation required for this project, Laser Analytics, which recently became a subsidiary of Spectra Physics. The change of ownership of the company considerably complicated our interaction with the prior management. A physical plant change took place at midyear. This was also accompanied by personnel policy changes in the company which have slowed our negotiations.

In spite of company advertisement of components which were needed to carry out the project, the white cell required had never been fabricated before. The manufacture of this instrument has required engineering modifications which have delayed the delivery of components.

At midyear the budget was modified to include capital equipment funds. This allowed us to proceed with the contract for final purchase. As of 30 September 1979 portions of the instrumentation have arrived at NRL but the complete system is not yet available for use. Some tests have been run with the spectrometer at the Laser Analytics Plant. Figure 17 shows a scan of a natural abundance CO_2 sample which contains the $^{13}CO_2$ P(24) line and the $^{12}CO_2$ R(60) line. This spectrum is measured with second derivative detection. The operation of the instrument appears to be excellent and we are very encouraged concerning its successful use for $^{14}CO_2$ when the system is operational at NRL.

4.4 PLANS FOR CARBON(14) MONITORING

When the instrumentation is operational at NRL it will be quality assurance tested. Immediately following its sensitivity for carbon (14) will be assessed and probable interfering gases will be analyzed.

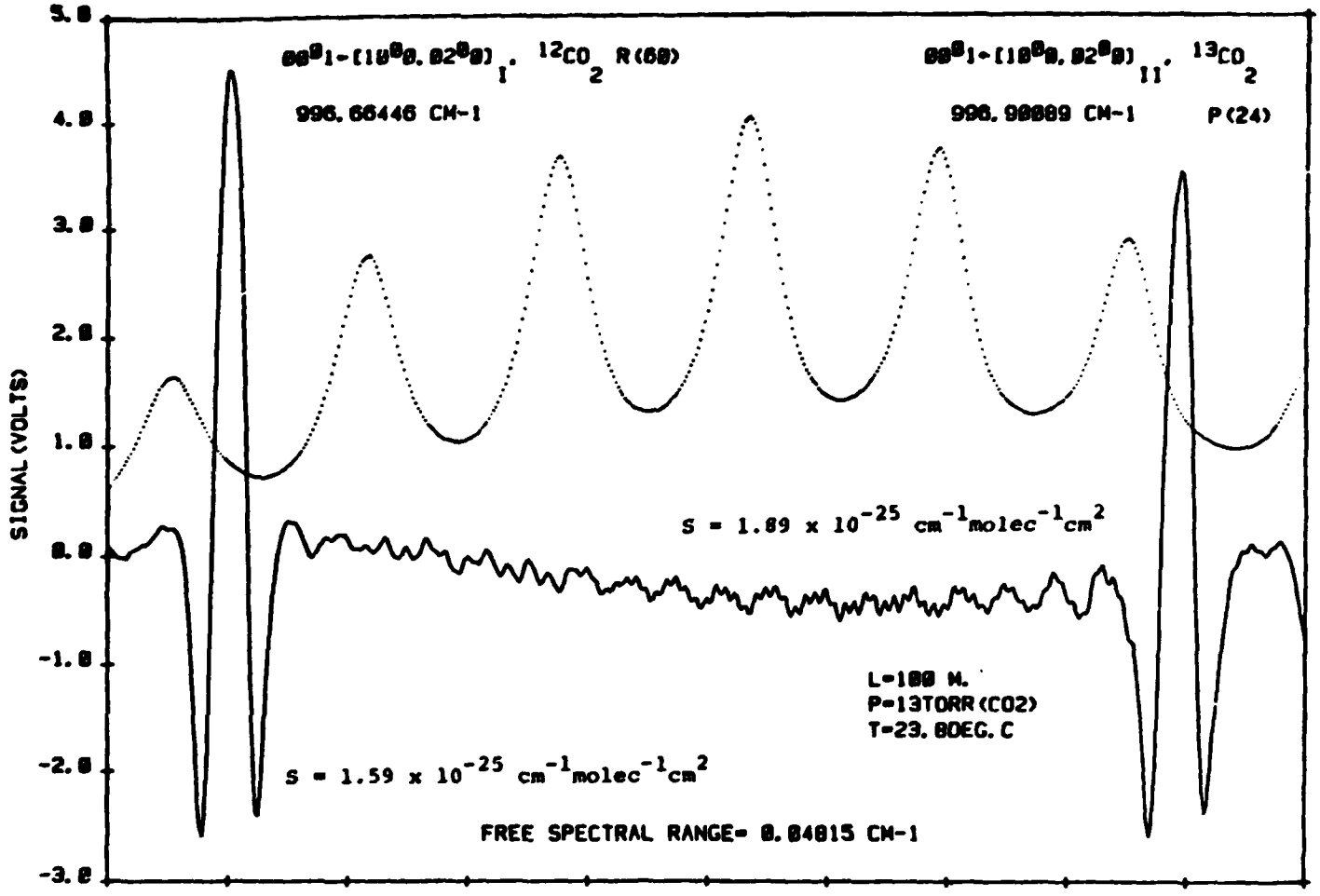

Fig. 17 - Laser diode spectrum of natural abundance $^{13}CO_2$ in $^{12}CO_2$. The solid line is the second derivative adsorption spectrum and the dotted line is an etalon spectrum used to accurately calibrate the frequencies of the absorption lines.

Provision has been made to receive from INEL in Idaho Falls air grab samples from available test points to be evaluated with the diode spectrometer.

NRL has proposed, that following the successful completion of these experiments, that routine grab samples from INEL test sites be analyzed on the instrument during FY80. This analytical service will provide a serious evaluation of the instrument and will provide routine monitoring information for carbon (14) release data at the INEL site over an extended period.

4.5 MONITORING OTHER ISOTOPES

We have explained in Section III of this document the plans for developing a capability for monitoring tritium in the form of HTO with this instrument. This will require extensive experimental time since the needed spectroscopic information for HTO is not available as it was for CO_2.

As time allows, we also plan to investigate the possibility of using the instrument for monitoring other isotopic species. These include ^{14}CO, $^{14}CH_4$, NO_2, and N_2O.

4.6 REFERENCES

1. "Carbon-14 Production in Nuclear Reactors"
   W. Davis, Jr.
   ORNL/NUREG/TM-12, February 1977.

2. "C-14 Gaseous Effluents from Pressurized Water Reactors"
   C. Kunz, W. E. Mahoney and T. W. Miller
   Health Physics Society, Symposium on Population Expenses, Knoxville, TN, October (1974).

3. "C-14 Gaseous Effluents from Boiling Water Reactors"
C. Kunz, W. E. Mahoney and T. W. Miller
Annual Meeting of the American Nuclear Society, New Orleans, LA, June 1975.

4. "Removal of ^{14}C - Contaminated CO_2 from Simulated LWR Full Reprocessing Off-Gas by Utilizing the Reaction Between CO_2 and Alkaline Hydroxides in Either Slurry or Solid Form"
D. W. Holladay and G. L. Haag
15th DoE Nuclear Air Cleaning Conference, Boston, MA, August 1978.

5. C. O. Kunz, W. E. Mahoney and T. W. Miller
Trans. Am. Nucl. Soc. 21, 91 (1975).

6. "Process Behavior of and Environmental Assessments of ^{14}C Releases from an HTGR Fuel Reprocessing Facility"
J. W. Snider and S. V. Kaye
Controlling Airborne Effluents from Fuel Cycle Plants, ANS-AeChE Meeting, Sun Valley, ID, August 1976.

7. "Nuclear Energy: Health Impact of Carbon-14"
R. O. Pohl
Rad. and Environm. Biophys. 13, 315 (1976).

8. "Production and Emission of Carbon-14 from Nuclear Power Stations and Reprocessing Plants and its Radiological Significance"
H. Bonka, K. Brusserman, G. Schwartz and V. Wollrodt
4th International Congress of the IRPA, Paris, April 1977.

9. "Monitoring and Removal of Gaseous Carbon-14 Species"
M. J. Kabot
15th DoE Nuclear Air Cleaning Conference, Boston, MA, August 1978.

10. "The Predicted Radiation Exposure of the Population of the European Community Resulting from Discharges of Krypton-85, Tritium, Carbon-14, and Iodine-129 from the Nuclear Power Industry in the Year 2000"
J. N. Kelly, J. A. Jones, P. M. Bryant and F. Morley
V/2676/75 Commission of the European Communities, Luxemburg, September 1975.

11. "Public Health Considerations of Carbon-14 Discharges from Light Water-Cooled Nuclear Power Reactor Industry"
T. W. Fowler, R. L. Clark, J. M. Gruheke and J. L. Russell
OPR/Tad-76-3, U.S.E.P.A., July 1976.

12. "Detection and Monitoring of Airborne Nuclear Waste Materials - Annual Report to the Department of Energy
J. R. McDonald, A. P. Baronavski, L. R. Pasternack-Rafferty, V. M. Donnelly and R. C. Clark
NRL Memorandum Report No. 3895, December 1978.